Astronomy & Astrophysics manuscript no. output
February 13, 2025
©ESO 2025

Appendix of: Catalogue of BRITE-Constellation targets⋆

I. Fields 1 to 14 (November 2013 – April 2016)

K. Zwintz[1], A. Pigulski[2], R. Kuschnig[3], G. A. Wade[4], G. Doherty[4], M. Earl[4], C. Lovekin[5], M. Müllner[1], S. Piché-Perrier[4], T. Steindl[1], P. G. Beck[3,6,7], K. Bicz[2], D. M. Bowman[8,9], G. Handler[10], B. Pablo[11], A. Popowicz[12], T. Różański[2], P. Mikołajczyk[2,13], D. Baade[14], O. Koudelka[15], A. F. J. Moffat[16], C. Neiner[17], P. Orleański[18], R. Smolec[10], N. St. Louis[16], W. W. Weiss[19], M. Wenger[15], and E. Zocłońska[10,20]

[1] Universität Innsbruck, Institut für Astro- und Teilchenphysik, Technikerstraße 25, 6020 Innsbruck, Austria
e-mail: konstanze.zwintz@uibk.ac.at
[2] Instytut Astronomiczny, Uniwersytet Wrocławski, Kopernika 11, 51-622 Wrocław, Poland
[3] Institut für Physik, Karl-Franzens Universität Graz, Universitätsplatz 5/II, NAWI Graz, 8010 Graz, Austria
[4] Department of Physics and Space Science, Royal Military College of Canada, PO Box 17000, Kingston, ON K7K 7B4, Canada
[5] Mount Allison University, 69 York St, Sackville, NB, Canada
[6] Instituto de Astrofísica de Canarias, 38200 La Laguna, Tenerife, Spain
[7] Departamento de Astrofísica, Universidad de La Laguna, 38206 La Laguna, Tenerife, Spain
[8] School of Mathematics, Statistics and Physics, Newcastle University, Newcastle upon Tyne, NE1 7RU, UK
[9] Institute of Astronomy, KU Leuven, Celestijnenlaan 200D, Leuven 3001, Belgium
[10] Nicolaus Copernicus Astronomical Center of the Polish Academy of Sciences, Bartycka 18, 00-716 Warsaw, Poland
[11] American Association of Variable Star Observers, 185 Alewife Brook Pkwy Suite. 410, Cambridge, MA 01238, USA
[12] Silesian University of Technology, Department of Electronics, Electrical Engineering and Microelectronics, Akademicka 16, 44-100 Gliwice, Poland
[13] Astronomical Observatory, University of Warsaw, Al. Ujazdowskie 4, 00-478 Warszawa, Poland
[14] European Organisation for Astronomical Research in the Southern Hemisphere (ESO), Karl-Schwarzschild-Str. 2, 85748 Garching b. München, Germany
[15] Technische Universität Graz, Inffeldgasse 12, 8010 Graz, Austria
[16] Département de physique, Université de Montréal, Campus MIL, 1375 Thérése-Lavoie-Roux, Montréal (Qc), Canada
[17] LESIA, Paris Observatory, PSL University, CNRS, Sorbonne University, Paris Cité University, 5 place Jules Janssen, 92195 Meudon, France
[18] Space Research Center, Polish Academy of Sciences, Bartycka 18A, 00-716 Warsaw, Poland
[19] University of Vienna, Department for Astrophysics, Türkenschanzstrasse 17, 1180 Vienna, Austria
[20] Łukasiewicz Research Network – Institute of Aviation, Al. Krakowska 110/114, 02-256 Warsaw, Poland

Received ; accepted

ABSTRACT

Here we provide the appendix of the publication "Catalogue of BRITE-Constellation targets I. Fields 1 to 14 (November 2013 – April 2016)" by Zwintz et al. 2024 (Astronomy & Astrophysics 683, 49).
This appendix contains the stars observed by BRITE-Constellation in fields 1 to 14 and the qualitative description of the individual data sets.
We also include a description of the format of the BRITE-Constellation data in the archives, plots of the data quality per satellite, and maps of the fields addressed in the publication.

Key words. Catalogs – Techniques: photometric – Methods: data analysis – Stars: general – Stars: variables: general

The full paper is accessible here: https://ui.adsabs.harvard.edu/abs/2024A%26A...683A..49Z/abstract.

⋆ Based on data collected by the BRITE-Constellation satellite mission, designed, built, launched, operated and supported by the Austrian Research Promotion Agency (FFG), the University of Vienna, the Technical University of Graz, the University of Innsbruck, the Canadian Space Agency (CSA), the University of Toronto Institute for Aerospace Studies (UTIAS), the Foundation for Polish Science & Technology (FNiTP MNiSW), and National Science Centre (NCN).

References

Abt, H. A. & Morrell, N. I. 1995, ApJS, 99, 135
Ake, T. B. & Parsons, S. B. 1987, Information Bulletin on Variable Stars, 3002, 1
Baade, D., Pigulski, A., Rivinius, T., et al. 2018a, A&A, 610, A70
Baade, D., Pigulski, A., Rivinius, T., et al. 2018b, A&A, 620, A145
Baade, D., Rivinius, T., Pigulski, A., et al. 2017, in Second BRITE-Constellation Science Conference: Small Satellites - Big Science, ed. K. Zwintz & E. Poretti, Vol. 5, 196–205
Baade, D., Rivinius, T., Pigulski, A., et al. 2016, A&A, 588, A56
Baade, D., Rivinius, T., Pigulski, A., et al. 2018c, in 3rd BRITE Science Conference, ed. G. A. Wade, D. Baade, J. A. Guzik, & R. Smolec, Vol. 8, 69–76
Bakos, G. A. 1974, AJ, 79, 866
Begy, S. B., Wade, G. A., Handler, G., et al. 2018, in 3rd BRITE Science Conference, ed. G. A. Wade, D. Baade, J. A. Guzik, & R. Smolec, Vol. 8, 154–158

Bidelman, W. P. 1951, ApJ, 113, 304
Borre, C. C., Baade, D., Pigulski, A., et al. 2020a, A&A, 635, A140
Borre, C. C., Baade, D., Pigulski, A., Weiss, A., & Rivinius, T. 2020b, in Stars and their Variability Observed from Space, ed. C. Neiner, W. W. Weiss, D. Baade, R. E. Griffin, C. C. Lovekin, & A. F. J. Moffat, 121–122
Bowman, D. M., Burssens, S., Pedersen, M. G., et al. 2019, Nature Astronomy, 3, 760
Burnashev, V. I. 1985, Abastumanskaia Astrofizicheskaia Observatoriia Byulleten, 59, 83
Buscombe, W. 1969, MNRAS, 144, 1
Buscombe, W. & Barkstrom, B. 1971, MNRAS, 152, 37
Buysschaert, B. & Neiner, C. 2016, in SF2A-2016: Proceedings of the Annual meeting of the French Society of Astronomy and Astrophysics, ed. C. Reylé, J. Richard, L. Cambrésy, M. Deleuil, E. Pécontal, L. Tresse, & I. Vauglin, 229–233
Buysschaert, B., Neiner, C., Martin, A. J., et al. 2019, A&A, 622, A67
Buysschaert, B., Neiner, C., Ramiaramanantsoa, T., et al. 2017a, in Second BRITE-Constellation Science Conference: Small Satellites - Big Science, ed. K. Zwintz & E. Poretti, Vol. 5, 101–108
Buysschaert, B., Neiner, C., Richardson, N. D., et al. 2017b, A&A, 602, A91
Conti, P. S. & Alschuler, W. R. 1971, ApJ, 170, 325
Corbally, C. J. 1984, ApJS, 55, 657
Cowley, A. 1972, AJ, 77, 750
Cowley, A., Cowley, C., Jaschek, M., & Jaschek, C. 1969, AJ, 74, 375
Cowley, A. P. 1968, PASP, 80, 453
Cowley, A. P. 1976, PASP, 88, 95
Cugier, H. & Pigulski, A. 2017, in Second BRITE-Constellation Science Conference: Small Satellites - Big Science, ed. K. Zwintz & E. Poretti, Vol. 5, 186–187
Danks, A. C. & Houziaux, L. 1978, PASP, 90, 453
Daszyńska-Daszkiewicz, J., Pamyatnykh, A. A., Walczak, P., et al. 2017a, MNRAS, 466, 2284
Daszyńska-Daszkiewicz, J., Walczak, P., Pamyatnykh, A., Jerzykiewicz, M., & Pigulski, A. 2017b, in Second BRITE-Constellation Science Conference: Small Satellites - Big Science, ed. K. Zwintz & E. Poretti, Vol. 5, 138–144
de Vaucouleurs, A. 1957, MNRAS, 117, 449
Elliott, A., Richardson, N. D., Pablo, H., et al. 2022, MNRAS, 509, 4246
Evans, D. S., Menzies, A., & Stoy, R. H. 1957, MNRAS, 117, 534
Evans, N. R. 1991, ApJ, 372, 597
Garrison, R. F. & Gray, R. O. 1994, AJ, 107, 1556
Gössl, S., Zwintz, K., & Kuschnig, R. 2017, in Second BRITE-Constellation Science Conference: Small Satellites - Big Science, ed. K. Zwintz & E. Poretti, Vol. 5, 236–239
Gray, R. O., Corbally, C. J., Garrison, R. F., et al. 2006, AJ, 132, 161
Gray, R. O. & Garrison, R. F. 1987, ApJS, 65, 581
Gray, R. O. & Garrison, R. F. 1989, ApJS, 70, 623
Handler, G. 2017, in Second BRITE-Constellation Science Conference: Small Satellites - Big Science, ed. K. Zwintz & E. Poretti, Vol. 5, 151–157
Handler, G., Pigulski, A., Weiss, W. W., et al. 2017a, in European Physical Journal Web of Conferences, Vol. 160, European Physical Journal Web of Conferences, 01001
Handler, G., Rybicka, M., Popowicz, A., et al. 2017b, MNRAS, 464, 2249
Hendry, E. M. 1981, AJ, 86, 271
Henry, T. J., Kirkpatrick, J. D., & Simons, D. A. 1994, AJ, 108, 1437
Hiltner, W. A., Garrison, R. F., & Schild, R. E. 1969, ApJ, 157, 313
Hiltner, W. A. & Schild, R. E. 1966, ApJ, 143, 770
Houk, N. 1978, Catalogue of two-dimensional spectral types for the HD stars. Vol. II. Declinations −53° to −40° (University of Michigan)
Houk, N. 1982, Catalogue of two-dimensional spectral types for the HD stars. Vol. III. Declinations −40° to −26° (University of Michigan)
Houk, N. & Cowley, A. P. 1975, Catalogue of two-dimensional spectral types for the HD stars. Vol. I. Declinations −90° to −53° (University of Michigan)
Huber, D. & Zwintz, K. 2020, in Stars and their Variability Observed from Space, ed. C. Neiner, W. W. Weiss, D. Baade, R. E. Griffin, C. C. Lovekin, & A. F. J. Moffat, 457–463
Jaschek, C. & Jaschek, M. 1965, PASP, 77, 376
Jaschek, M. & Jaschek, C. 1959, PASP, 71, 48
Jerzykiewicz, M., Pigulski, A., Handler, G., et al. 2020, MNRAS, 496, 2391
Jerzykiewicz, M., Pigulski, A., Michalska, G., et al. 2021, MNRAS, 503, 5554
Johnson, H. L. & Morgan, W. W. 1953, ApJ, 117, 313
Kallinger, T., Beck, P. G., Hekker, S., et al. 2019, A&A, 624, A35
Kallinger, T. & Weiss, W. W. 2017, in Second BRITE-Constellation Science Conference: Small Satellites - Big Science, ed. K. Zwintz & E. Poretti, Vol. 5, 113–119
Kallinger, T. & Weiss, W. W. 2018, in 3rd BRITE Science Conference, ed. G. A. Wade, D. Baade, J. A. Guzik, & R. Smolec, Vol. 8, 170–174
Kallinger, T., Weiss, W. W., Beck, P. G., et al. 2017, A&A, 603, A13
Keenan, P. C. & McNeil, R. C. 1989, ApJS, 71, 245
Keenan, P. C. & Morgan, W. W. 1941, ApJ, 94, 501
Keenan, P. C. & Pitts, R. E. 1980, ApJS, 42, 541
Keenan, P. C., Yorka, S. B., & Wilson, O. C. 1987, PASP, 99, 629
Kenworthy, M. A., Mellon, S. N., Bailey, J. I., et al. 2021, A&A, 648, A15
Kondrak, M., Przybilla, N., Zwintz, K., & Crires-Pop Collaboration. 2017, in Second BRITE-Constellation Science Conference: Small Satellites - Big Science, ed. K. Zwintz & E. Poretti, Vol. 5, 240–246
Kraft, R. P. 1960, ApJ, 131, 330
Krtička, J. & Feldmeier, A. 2018, A&A, 617, A121
Krtička, J., Huang, L., Jagelka, M., et al. 2018, Contributions of the Astronomical Observatory Skalnate Pleso, 48, 170
Krtička, J., Mikulášek, Z., Prvák, M., et al. 2020, MNRAS, 493, 2140
Landi Dessy, J. & Keenan, P. C. 1966, ApJ, 146, 587
Lesh, J. R. 1968, ApJS, 17, 371
Levato, O. H. 1972, PASP, 84, 584
Lovekin, C. & Tompkins, J. 2020, in Stars and their Variability Observed from Space, ed. C. Neiner, W. W. Weiss, D. Baade, R. E. Griffin, C. C. Lovekin, & A. F. J. Moffat, 99–100
Maíz Apellániz, J., Barbá, R. H., Simón-Díaz, S., et al. 2018, A&A, 615, A161
Malaroda, S. 1973, PASP, 85, 328
Malaroda, S. 1975, AJ, 80, 637
Moffat, A. F. J., St-Louis, N., Carlos-Leblanc, D., et al. 2018, in 3rd BRITE Science Conference, ed. G. A. Wade, D. Baade, J. A. Guzik, & R. Smolec, Vol. 8, 37–42
Mol Lous, M., Weenk, E., Kenworthy, M. A., Zwintz, K., & Kuschnig, R. 2018, A&A, 615, A145
Morgan, W. W., Code, A. D., & Whitford, A. E. 1955, ApJS, 2, 41
Morgan, W. W. & Keenan, P. C. 1973, ARA&A, 11, 29
Morgan, W. W. & Roman, N. G. 1950, ApJ, 112, 362
Morris, P. M. 1961, MNRAS, 122, 325
Moździerski, D. & Pigulski, A. 2016, in 37th Meeting of the Polish Astronomical Society, ed. A. Różańska & M. Bejger, Vol. 3, 98–101
Nassau, J. J. & van Albada, G. B. 1947, ApJ, 106, 20
Niemczura, E., Pigulski, A., Kamińska, M. K., et al. 2018, in XXXVIII Polish Astronomical Society Meeting, ed. A. Ró&żańska, Vol. 7, 162–167
Niemczura, E., Pigulski, A., Lehmann, H., et al. 2017, in Second BRITE-Constellation Science Conference: Small Satellites - Big Science, ed. K. Zwintz & E. Poretti, Vol. 5, 217–218
Oplištilová, A., Harmanec, P., Mayer, P., et al. 2020, Contributions of the Astronomical Observatory Skalnate Pleso, 50, 585
Oplištilová, A., Mayer, P., Harmanec, P., et al. 2023, A&A, 672, A31
Pablo, H., Richardson, N. D., Fuller, J., Moffat, A. F. J., & Photometry Tiger Team (Phott). 2017a, in Second BRITE-Constellation Science Conference: Small Satellites - Big Science, ed. K. Zwintz & E. Poretti, Vol. 5, 167–172
Pablo, H., Richardson, N. D., Fuller, J., et al. 2017b, MNRAS, 467, 2494
Pablo, H., Richardson, N. D., & Moffat, A. F. J. 2018, in 3rd BRITE Science Conference, ed. G. A. Wade, D. Baade, J. A. Guzik, & R. Smolec, Vol. 8, 101–105
Pablo, H., Shultz, M., Fuller, J., et al. 2019, MNRAS, 488, 64
Parsons, S. B. & Ake, T. B. 1998, ApJS, 119, 83
Paunzen, E. & Rode-Paunzen, M. 2017, in Second BRITE-Constellation Science Conference: Small Satellites - Big Science, ed. K. Zwintz & E. Poretti, Vol. 5, 180–185
Pigulski, A., Cugier, H., Handler, G., & Kgoadi, R. 2018a, in 3rd BRITE Science Conference, ed. G. A. Wade, D. Baade, J. A. Guzik, & R. Smolec, Vol. 8, 77–79
Pigulski, A., Cugier, H., Popowicz, A., et al. 2016, A&A, 588, A55
Pigulski, A., Jerzykiewicz, M., Ratajczak, M., Michalska, G., & Zahajkiewicz, E. 2017, in Second BRITE-Constellation Science Conference: Small Satellites - Big Science, ed. K. Zwintz & E. Poretti, Vol. 5, 120–127
Pigulski, A., Kamińska, M. K., Kamiński, K., et al. 2018b, in 3rd BRITE Science Conference, ed. G. A. Wade, D. Baade, J. A. Guzik, & R. Smolec, Vol. 8, 115–117
Popowicz, A., Pigulski, A., Bernacki, K., et al. 2017, A&A, 605, A26
Ramiaramanantsoa, T. & Moffat, A. F. J. 2020, in Stars and their Variability Observed from Space, ed. C. Neiner, W. W. Weiss, D. Baade, R. E. Griffin, C. C. Lovekin, & A. F. J. Moffat, 147–153
Ramiaramanantsoa, T., Moffat, A. F. J., Harmon, R., et al. 2018a, MNRAS, 473, 5532
Ramiaramanantsoa, T., Ratnasingam, R., Shenar, T., et al. 2018b, MNRAS, 480, 972
Ratajczak, M. & Pigulski, A. 2018, in 3rd BRITE Science Conference, ed. G. A. Wade, D. Baade, J. A. Guzik, & R. Smolec, Vol. 8, 118–122
Ratajczak, M., Pigulski, A., & Pavlovski, K. 2019, Contributions of the Astronomical Observatory Skalnate Pleso, 49, 252
Rauw, G., Pigulski, A., Nazé, Y., et al. 2019, A&A, 621, A15
Richardson, N., Moffat, A., St-Louis, N., et al. 2017a, in Second BRITE-Constellation Science Conference: Small Satellites - Big Science, ed. K. Zwintz & E. Poretti, Vol. 5, 55–60
Richardson, N. D., Russell, C. M. P., St-Jean, L., et al. 2017b, MNRAS, 471, 2715

Roman, N. G. 1952, ApJ, 116, 122
Rybicka, M. 2017, in Second BRITE-Constellation Science Conference: Small Satellites - Big Science, ed. K. Zwintz & E. Poretti, Vol. 5, 163–166
Rybicka, M., Zocłońska, E., & Tomić, S. 2018, in 3rd BRITE Science Conference, ed. G. A. Wade, D. Baade, J. A. Guzik, & R. Smolec, Vol. 8, 134–138
Schmutz, W. & Koenigsberger, G. 2019, A&A, 624, L3
Slettebak, A. 1955, ApJ, 121, 653
Slettebak, A. 1963, ApJ, 138, 118
Slettebak, A. 1982, ApJS, 50, 55
Smalley, B., Paunzen, E., Lüftinger, T., et al. 2018, Bulgarian Astronomical Journal, 28, 27
Smith, L. F. 1968, MNRAS, 138, 109
Smolec, R., Moskalik, P., Evans, N. R., Moffat, A. F. J., & Wade, G. A. 2017, in Second BRITE-Constellation Science Conference: Small Satellites - Big Science, ed. K. Zwintz & E. Poretti, Vol. 5, 265–271
Smolec, R., Moskalik, P., Evans, N. R., Moffat, A. F. J., & Wade, G. A. 2018, in 3rd BRITE Science Conference, ed. G. A. Wade, D. Baade, J. A. Guzik, & R. Smolec, Vol. 8, 88–93
Sota, A., Maíz Apellániz, J., Morrell, N. I., et al. 2014, ApJS, 211, 10
Sota, A., Maíz Apellániz, J., Walborn, N. R., et al. 2011, ApJS, 193, 24
St-Louis, N., Moffat, A. F. J., Ramiaramanantsoa, T., & Lenoir-Craig, G. 2020, in Stars and their Variability Observed from Space, ed. C. Neiner, W. W. Weiss, D. Baade, R. E. Griffin, C. C. Lovekin, & A. F. J. Moffat, 423–426
Sterken, C., Vogt, N., & Mennickent, R. 1994, A&A, 291, 473
Struve, O. & Sahade, J. 1957, ApJ, 125, 689
van Leeuwen, F. & van Genderen, A. M. 1997, A&A, 327, 1070
Wade, G. A., Cohen, D. H., Fletcher, C., et al. 2017, in Second BRITE-Constellation Science Conference: Small Satellites - Big Science, ed. K. Zwintz & E. Poretti, Vol. 5, 94–100
Wade, G. A., Pigulski, A., Begy, S., et al. 2020, MNRAS, 492, 2762
Walborn, N. R. 1972, AJ, 77, 312
Walczak, P., Daszyńska-Daszkiewicz, J., Pamyatnykh, A., Handler, G., & Pigulski, A. 2017, in Second BRITE-Constellation Science Conference: Small Satellites - Big Science, ed. K. Zwintz & E. Poretti, Vol. 5, 173–179
Walczak, P., Daszyńska-Daszkiewicz, J., Pigulski, A., et al. 2019, MNRAS, 485, 3544
Weiss, W. W., Fröhlich, H. E., Kallinger, T., et al. 2020, A&A, 642, A64
Weiss, W. W., Fröhlich, H. E., Pigulski, A., et al. 2016, A&A, 588, A54
Weiss, W. W., Zwintz, K., Kuschnig, R., et al. 2021, Universe, 7, 199
Wilson, R. E. & Joy, A. H. 1950, ApJ, 111, 221
Yamashita, Y. 1967, Publications of the Dominion Astrophysical Observatory Victoria, 13, 47
Yeh, L.-C. & Jiang, I.-G. 2021, PASP, 133, 014401
Zocłońska, E. 2017, in Second BRITE-Constellation Science Conference: Small Satellites - Big Science, ed. K. Zwintz & E. Poretti, Vol. 5, 158–162
Zocłońska, E. 2018, in 3rd BRITE Science Conference, ed. G. A. Wade, D. Baade, J. A. Guzik, & R. Smolec, Vol. 8, 94–98
Zwintz, K. 2017, in Second BRITE-Constellation Science Conference: Small Satellites - Big Science, ed. K. Zwintz & E. Poretti, Vol. 5, 228–235
Zwintz, K. 2018, in 3rd BRITE Science Conference, ed. G. A. Wade, D. Baade, J. A. Guzik, & R. Smolec, Vol. 8, 161–164
Zwintz, K., Kuschnig, R., Arnold, C., et al. 2020a, in Stars and their Variability Observed from Space, ed. C. Neiner, W. W. Weiss, D. Baade, R. E. Griffin, C. C. Lovekin, & A. F. J. Moffat, 119–120
Zwintz, K., Neiner, C., Kochukhov, O., & Ryabchikova, T. 2019a, in Astronomical Society of the Pacific Conference Series, Vol. 518, Physics of Magnetic Stars, ed. D. O. Kudryavtsev, I. I. Romanyuk, & I. A. Yakunin, 59
Zwintz, K., Neiner, C., Kochukhov, O., et al. 2020b, A&A, 643, A110
Zwintz, K., Reese, D. R., Neiner, C., et al. 2019b, A&A, 627, A28
Zwintz, K., Van Reeth, T., Tkachenko, A., et al. 2017, A&A, 608, A103

Appendix A: BRITE-Constellation targets in the first 14 fields

Table A.1 provides an overview of the 300 stars observed by BRITE-Constellation included in the first 14 fields. The columns used are HD identifier (HD), other commonly used identifier (Other designation), V magnitude (V) and spectral classification with references (MK spectral type). The BRITE field numbers in which the star was observed are then given (BRITE field(s)). Numbers in brackets indicate fields from which data will be discussed in subsequent papers. In the two columns entitled 'Class of variability', we list the variability type assigned in the VSX database and the classification based on the BRITE-Constellation data. We follow the classification scheme used in the VSX database.[1] The last column in Table A.1 provides the publications that used BRITE-Constellation data for presented stars and notes on the objects. In a few cases, two HD numbers are given in one line, which may be due to one of two reasons: either these are visual double stars that were not resolved in the BRITE photometry (e.g. for HD 36861/2), or a single star was given two HD numbers in the original catalogue (e.g. for HD 195068/9).

[1] A description of the VSX variability types is available at https://www.aavso.org/vsx/index.php?view=about.vartypes.

Table A.1: General information on the 300 BRITE-Constellation target stars included in Fields 1 to 14.

HD	Other designation	V (mag)	MK spectral type	BRITE field(s)	Variability class VSX	Variability class this paper	Notes, references to BRITE papers
432	β Cas	2.27	F2 IV [1]	11 (19,30,39,57)	DSCTC	DSCT	(28,61,75)
2905	κ Cas	4.16	B1 Ia [2]	11 (19,30,39,57)	ACYG	ACYG	(21,46)
3360	ζ Cas	3.66	B2 IV [3]	11 (19,30,39)	—	SPB	
3712	α Cas	2.23	K0 IIIa [4]	11 (19)	ROT:	—	
3901	ξ Cas	4.81	B2 V [1]	11	—	—	
4614	η Cas	3.44	G0 V + K7 V [4,5]	11 (19)	CST	—	
5394	γ Cas	2.47	B0 IV:e [6]	11 (19,30,39,57)	GCAS+X+LERI:	GCAS+SPB	(26,64,70)
6811	ϕ And	4.25	B7 III [7]	11	BE:	—	
6961	θ Cas	4.33	A7 IV [8]	11 (19,30,39)	—	—	
8538	δ Cas	2.68	A5 IV [9]	11 (19,30,39)	EA:	—	
11415	ε Cas	3.37	B3 Vp shell [10]	11 (19,30,39)	SXARI:	BE	
16908	35 Ari	4.66	B3 V [10]	5	n.e.	—	
17573	41 Ari	3.63	B8 Vn [7]	5	—	—	
17584	16 Per	4.23	F2 III [1]	5	DSCT:	DSCT	
17709	17 Per	4.53	K7 III [3]	5	LB	—	
18296	21 (LT) Per	5.11	B9p Si [8]	5	ACV	VAR	
19058	ρ Per	3.39	M4 II [4]	5	SRB	VAR	(57)
19356	β Per	2.12	B8 V + A/F [11]	5	EA/SD	E	
19373	ι Per	4.05	G0 V [4]	5	n.e.	—	
19476	κ Per	3.80	K0 III [3]	5	—	—	
20365	29 Per	5.15	B3 V [10]	5	n.e.	—	α Per, (4)
20418	31 Per	5.03	B5 IV [10]	5	n.e.	—	α Per, (4)
20468	—	4.82	K2 II CN0.5 [12]	5	n.e.	—	
20809	—	5.29	B4 IV [10]	5	SPB:	VAR	α Per, (4)
20902	α Per	1.79	F5 Ib [2]	5	—	—	α Per
21428	34 Per	4.67	B5 V [10]	5	n.e.	—	α Per, (4)
21552	σ Per	4.36	K3 III [13]	5	LB	VAR	(57)
22192	ψ Per	4.23	B5 Ve [10]	5	GCAS	SPB	α Per, (4)
22780	—	5.57	B7 Vn [10]	5	GCAS:	—	
22928	δ Per	3.01	B5 III [10]	5 (20)	GCAS:	VAR	
23180	o Per	3.83	B1 III [3]	5	ELL	VAR	(21,46)
23230	ν Per	3.77	F5 II [2]	5 (20)	—	—	
23302	17 Tau	3.70	B6 III [1]	5	SPB	—	Pleiades
23338	19 Tau	4.30	B6 V [1]	5	SPB	—	Pleiades
23408	20 Tau	3.87	B7 III [1]	5	ACV	VAR	Pleiades
23480	23 (V971) Tau	4.18	B6 IVnn	5	SPB | LERI	—	Pleiades
23630	η Tau	2.87	B7 III [3]	5	ROT+SPB	BE	Pleiades
23850	27 Tau	3.63	B8 III [1]	5	SPB	SPB	Pleiades, (49)
24398	ζ Per	2.85	B1 Ib [2]	5 (20)	—	ACYG	(21,46)
24640	—	5.49	B1.5 V [10]	5	BCEP:	—	
24760	ε Per	2.89	B0.5 III [10]	5 (20)	BCEP	BCEP+SPB	(20,42)
24912	ξ Per	4.04	O7.5 III((f))(n) [14]	5 (20)	*	VAR	
25823	41 (GS) Tau	5.20	B9 Vp Si [8]	5	ACV	VAR	
25940	48 (MX) Per	4.04	B3 Ve [10]	5 (20)	GCAS	VAR	
25998	50 (V582) Per	5.51	F7 V [15]	5	RS:	—	
26322	44 (IM) Tau	5.41	F3 V [15]	5	DSCT	DSCT	
26630	μ Per	4.14	G0 Ib [2]	5 (20)	—	—	
27396	53 (V469) Per	4.85	B4 IV [10]	5 (20)	SPB	SPB	(27,51)
29248	ν Eri	3.93	B2 III [10]	6,13 (22,32,40,49,58,59,65)	BCEP+SPB	BCEP+SPB	(6,7,11,19,23)
30211	μ Eri	4.02	B4 IV [10]	6,13 (22,32,40,49,59,65)	EA+SPB	E+SPB	
30652	π^3 Ori	3.19	F6 V [3]	6,(40,65)	—	—	
30836	π^4 Ori	3.69	B2 III [1]	6,13 (22,32,40,49,58,59,65)	VAR	VAR	
31109	ω Eri	4.39	A9 IVn [16]	6	GDOR+DSCT	VAR	
31139	5 Ori	5.33	M1 III [17]	6	—	VAR	
31237	π^5 Ori	3.72	B2 III [10]	1,6,13 (22,32,40,49,58,59,65)	ELL	ELL+SPB	(67)
31767	π^6 Ori	4.47	K2 II [2]	6 (58)	—	—	
33111	β Eri	2.79	A3 III [18]	1,6 (32,40,48,58)	—	VAR	
33328	λ Eri	4.27	B2 III(e)p [19]	6,13 (22,32)	LERI+GCAS	VAR	
33904	μ Lep	3.31	B9p HgMn [8]	6	ACV	—	
34085	β Ori	0.12	B8 Ia [2]	1,6,13 (22,32,40,49,59,65)	ACYG	VAR	
34503	τ Ori	3.60	B5 III [1]	1,6,13 (22,49,59,65)	n.e.	HB	(44)
34816	λ Lep	4.29	B0.5 IV [6]	6 (22)	n.e.	VAR	
35039	22 Ori	4.74	B2 IV-V [10]	6 (40,49,59,65)	BCEP:	—	
35369	29 Ori	4.14	G8 III [13]	6	n.e.	—	
35411	η Ori	3.36	B0.7 V + B1.5: V [20]	1,6,13 (22,32,40,49,58,59,65)	EA+BCEP:	E+ELL	(17)
35439	ψ^1 Ori	4.95	B1 V:ep [6]	6,13 (22,32,40,49,58,59,65)	GCAS	BE+SPB	(26,39)
35468	γ Ori	1.64	B2 III [1]	1,6,13 (22,32,40,49,59,65)	—	—	
35715	ψ^2 Ori	4.59	B1 V [10]	1,6 (22,32,40,49,59,65)	E/D	ELL+BCEP	(17)
36267	32 Ori	4.20	B5 V [10]	6 (32,40,65)	n.e.	VAR	
36486/5	δ^1/δ^2 Ori	2.23/6.83	O9.5 II-III + B2 IV-V [10]	1,6,13 (22,32,40,48,49,58,59,65)	EA+VAR:	E+VAR	(65,79)
36512	υ Ori	4.62	B0 V [10]	6	BCEPS:	—	
36822	ϕ^1 Ori	4.41	B0.5 IV-V [10]	6 (40,58)	n.e.	—	
36861/2	λ^1/λ^2 Ori	3.54/5.45	O8 IIIf + B0.5 V [21]	1,6,13 (22,32,40,48,58,65)	—	—	
36960/59	—	5.67/4.78	B0.5 V + B1 V [10]	6	VAR:	—	
37018	42 Ori	4.59	B1 V [10]	6 (49,65)	CST	—	
37022/41	θ^1/θ^2 Ori	5.13/5.09	O6pe + O9.5 Vpe [10]	6,13	—	VAR	
37043	ι Ori	2.77	O8.5 III + B0 [21]	1,6,13 (22,32,49,58,59,65)	HB	HB	(8,11,22)
37128	ε Ori	1.70	B0 Ia [2]	1,6,13 (22,32,40,48,49,58,59,65)	ACYG	ACYG	(52)

Table A.1: continued.

HD	Other designation	V (mag)	MK spectral type	BRITE field(s)	Variability class VSX	Variability class this paper	Notes, references to BRITE papers
37468	σ Ori	3.81	O9.5 V [10]	1,6,13 (22,32,40,49,58,59,65)	VAR:	VAR	(76)
37490	ω Ori	4.57	B2 III(e) [10]	6,13 (22,32,40,58)	GCAS	VAR	(26)
37742/3	ζ Ori A/B	1.88/3.70	O9.5 Ib + O9.5 [2]	1,6,13 (22,32,40,48,49,58,59,65)	VAR	ACYG	(5,9,15)
38771	κ Ori	2.06	B0.5 Ia [2]	1,6,13 (22,32,49,59,65)	ACYG	ACYG	
39060	β Pic	3.85	A5 IV shell [19]	8 (23,33,50,61)	DSCT+EP:	DSCT	(28,37,48,60)
39801	α Ori	0.50	M2 Iab [2]	1,6,13 (22,32,40,49,59,65)	SRC	VAR	
42933	δ Pic	4.81	B0.5 IV [23]	8 (23,33,50,61)	EB/D:	E+BCEP	(17)
44402	ζ CMa	3.02	B2.5 IV [23]	12	BCEP:	VAR	
44743	β CMa	1.98	B1 II-III [10]	12	BCEP	BCEP	(19)
45348	α Car	−0.72	F0 Iab [24]	8 (23)	n.e.	—	
45871	IY CMa	5.74	B5 V(e) [19]	12	E:	VAR	
46328	ξ^1 CMa	4.33	B0.5 IV [6]	12	BCEP	BCEP	(19,47,63)
47306	N Car	4.40	A0 II [25]	8 (23)	n.e.	—	
47670	ν Pup	3.17	B8 III [26]	8 (23,33,41,50,61)	LERI	SPB+BE	(53)
48917	10 (FT) CMa	5.20	B2 IIIe [23]	12	GCAS	BE	(26)
49131	HP CMa	5.80	B1.5 Vne [27]	12	GCAS+LERI	—	
50013	κ CMa	3.96	B1.5 IVne [23]	12 (41)	GCAS	BE	(26)
50123	HZ CMa	5.70	B6 IVe + A [19]	12	ELL	ELL	
50337	V415 Car	4.42	G6 II + A0 V [28,29]	8 (33,50,61,66)	EA/GS	—	
50707	15 (EY) CMa	4.83	B1 IV [6]	12	BCEP	BCEP	(19)
50877	o^1 CMa	3.87	K3 Iab [2]	12	LC	VAR	
50896	EZ CMa	6.91	WN5-B [30]	12	WR	ROT+WR	WR 6, (13,38,56,72)
51309	ι CMa	4.37	B3 II [2]	12	BCEP	BCEP	
52089	ε CMa	1.50	B2 II [2]	12 (41)	n.e.	VAR	(14)
52670	LS CMa	5.63	B2 V [23]	12	EA+SPB	E	(59)
52877	σ CMa	3.47	K7 Ib [3]	12 (41)	LC	VAR	(57)
53138	o^2 CMa	3.02	B3 Ia [2]	12 (41)	ACYG	VAR	
53244	γ CMa	4.12	B8 II [10]	12	—	—	
54309	FV CMa	5.71	B2 IVe [23]	12	GCAS	—	
54605	δ CMa	1.84	F8 Ia [2]	12 (41)	VAR	—	
55892	71 (QW) Pup	4.49	F0 IV [31]	8 (23,33,50,61,66)	GDOR	GDOR	(28,69)
56014	27 (EW) CMa	4.66	B3 IVe [32]	12 (41)	GCAS	BE+SPB	(26)
56022	72 (OU) Pup	4.87	Ap SiSr [18]	8 (23,61)	ACV	—	
56139	ω CMa	3.85	B3 IVe [33]	12 (41)	GCAS	BE	(26)
56455	PR Pup	5.71	Ap Si [34]	8	ACV	VAR	
56855	π Pup	2.70	K4 III + B5 [35,36]	8 (33,41,50,61,66)	SRD:	—	
57060	29 (UW) CMa	4.98	O8.5 If [21]	12 (41)	EB/KE:	E+VAR	(43)
57061	τ CMa	4.40	O9 III [1]	12 (41)	EB	E	in NGC 2362
58155	NO CMa	5.43	B3 IV(e) [33]	12	BE:	VAR	
58286	—	5.39	B2 V [23]	12	n.e.	—	
58343	FW CMa	5.33	B2.5 V(e) [10]	12	GCAS	VAR	(26)
58350	η CMa	2.45	B5 Ia [2]	12 (41)	ACYG	VAR	
61068	PT Pup	5.74	B2 III [6]	12	BCEP	BCEP+SPB	(19)
61715	MY Pup	5.68	F7 Ib/II [37]	8 (23,33,50,61)	DCEPS	DCEPS	(31,41)
62623	3 Pup	3.96	A2 Iab [23]	12 (41)	ACYG	ACYG	
62747	V390 Pup	5.60	B1.5 III [23]	12	EA	E	
63462	o Pup	4.50	B1 Ve [24]	12	LERI:	VAR	
63744	Q Pup	4.71	K0 III [38]	7	n.e.	—	
63922	P Pup	4.11	B0.5 III [24]	7,8 (23,50,61)	n.e.	—	
63949	QS Pup	5.81	B1.5 IV [23]	8 (23,33)	BCEP	—	
64440	a Pup	3.73	K1.5 II + A [37]	7,8 (34,41,42,50,61,66)	n.e.	VAR	
64740	—	4.63	B1.5 IVp [23]	7,8,14 (23,25,66)	—	VAR	
64760	J Pup	4.24	B0.5 Ib [23]	7,8,14 (23,25,33,50,61)	VAR	VAR	
65575	χ Car	3.47	B3 IVp Si [23]	7,8,14 (23,25,33,34,42,50,51,61,66)	BCEP	VAR	
65818	V Pup	4.41	B1 Vp + B2: [23]	7,8,14 (23,25,33,50,61,66)	EB/SD	E	(17)
66811	ζ Pup	2.25	O4 I(n)fp [39]	7,8,14 (23,25,34,41,42,50,51,60,61,66)	ROT:	ROT+ACYG	(33,71)
67523	ρ Pup	2.81	F6 II [40]	12 (41)	DSCT	DSCT	
68273/43	γ^2/γ^1 Vel	4.20/1.83	WC8 + O7 + B1 IV [41,23]	7,8,14 (23,25,34,42,51,60,66)	WR	WR	WR 11, (12,13,38)
68553	h^1 (NS) Pup	4.45	K4 III [42]	7	LC	VAR	(57)
69142	h^2 Pup	4.44	K1 II/III [37]	7	n.e.	—	
71129	ε Car	2.01	K3: III + B2: V [28]	7 (25,34,42,51,60)	E:	VAR	
72127	—	4.99	B2 IV [23]	7	VAR:	—	
73634	e Vel	4.14	A9 I-II [24]	7 (25,66)	n.e.	—	
74006	β Pyx	3.97	G5 II/III [42]	7 (34,42)	n.e.	VAR	(57)
74180	b Vel	3.84	F2 Ia [40]	7 (25,66)	—	—	
74195	o Vel	3.62	B3 III [24]	7,14 (25,34,42,51,66)	SPB	SPB	
74375	d (V343) Car	4.33	B1 III [24]	7 (24,25,34,36,42,43,51)	BCEP:	VAR	
74560	HY Vel	4.86	B4 IV [43]	7	SPB	VAR	in IC 2391
74575	α Pyx	3.68	B1.5 III [23]	7	BCEP	VAR	
74772	d Vel	4.07	G5 III [37]	7	n.e.	—	
74956	δ Vel	1.96	A1 V [18]	7 (25,34,42,51,60,66)	EA	E	(59)
75063	a Vel	3.91	A1 III [18]	7	n.e.	VAR	
75311	f (V344) Car	4.49	B3 Vne [24]	7,14 (24,25,36,43,53,62,67)	GCAS	BE	
75821	f (KX) Vel	5.12	B0 III [6]	7	EA	—	
76728	c Car	3.84	B8 II [24]	7,14 (24,25,34,42,51)	n.e.	VAR	
77002	b^1 (V376) Car	4.89	B3 IV [24]	7	BCEPS	—	
78004	c Vel	3.75	K2 III [40]	7	n.e.	—	

Table A.1: continued.

HD	Other designation	V (mag)	MK spectral type	BRITE field(s)	Variability class VSX	Variability class this paper	Notes, references to BRITE papers
78647	λ Vel	2.21	K4 Ib [44]	7 (25,34,42)	LC	VAR	
79351	a (V357) Car	3.44	B2 IV [24]	7,14 (24,25,34,36,42,43,51,53)	BE:	SPB	(18)
79940	k Vel	4.62	F5 III [24]	7	n.e.	—	
80230	g Car	4.34	M1 III [28]	7 (24)	—	VAR	(57)
80404	ι Car	2.25	F0 Iab [24]	7,14 (24,25,34,42,51)	—	VAR	(30)
81188	κ Vel	2.50	B2 IV [24]	7,14 (24,25,34,36,42,51,53,60)	n.e.	SPB	(18)
82434	ψ Vel	3.60	F2 IV [24]	7	n.e.	—	
82668	N Vel	3.13	K5 III [35]	7 (24,25,34,36,42,43)	SR	VAR	(57)
83183	h Car	4.08	B5 II [23]	7 (24,36,53)	—	—	
83446	M Vel	4.35	A5 V [18]	7 (36,43)	n.e.	DSCT	(28)
86440	ϕ Vel	3.54	B5 II [24]	7 (24,36,43,53)	n.e.	—	
118716	ε Cen	2.30	B1 III [23]	2 (15,35)	BCEP	BCEP	(20)
120307	ν Cen	3.41	B2 IV [23]	2 (35)	R	R	(17,77)
120324	μ Cen	3.04	B2 IV-Ve [19]	2 (35)	GCAS	BE	(3,11)
121263	ζ Cen	2.55	B2.5 IV [23]	2 (15,35)	VAR	HB	(11)
121743	ϕ Cen	3.83	B2 IV [23]	2 (35)	—	VAR	
121790	υ^1 Cen	3.87	B2 IV-V [23]	2 (35)	L	—	(24)
122451	β Cen	0.61	B1 III [23]	2 (15,35,62)	BCEP	BCEP+SPB	(2,11,68)
122980	χ Cen	4.36	B2 V [23]	2 (35)	BCEPS	—	(24)
125238	ι Lup	3.55	B2.5 IV [23]	2 (35)	BCEP:	VAR	
125823	a (V761) Cen	4.42	B7 IIIp [23]	2 (35)	SXARI	ROT	(14,35,66)
126341	τ^1 Lup	4.56	B2 IV [23]	2 (35)	BCEP	BCEP+SPB	(25)
126354	τ^2 Lup	4.35	F4 IV + A7: [45]	2	n.e.	VAR	
127381	σ Lup	4.42	B2 III [23]	2 (35)	SXARI	VAR	
127972/3	η Cen	2.31	B2 Vnne [46]	2 (35)	GCAS+LERI	BE	(3,11)
128345	ρ Lup	4.05	B5 V [23]	2 (35)	SPB:	VAR	
128620/1	α Cen	−0.01	G2 V + K1 V [28]	2 (15,35,62)	BY:	VAR	(73)
128898	α Cir	3.19	Ap SrEuCr: [28]	2 (15,35,62)	roAp+ACV	roAp+ACV	(1,11,74)
129056	α Lup	2.30	B1.5 III [23]	2 (35)	BCEP	BCEP+SPB	(19,23)
129116	b Cen	4.00	B3 V [23]	2	n.e.	—	(24)
130807	o Lup	4.32	B5 IV [23]	2 (35)	VAR:	SPB+ROT	(55)
132058	β Lup	2.68	B2 III [23]	2 (35)	n.e.	SPB	(25)
132200	κ Cen	3.13	B2 IV [23]	2 (35)	BCEP	SPB	(18)
133242/3	π Lup	4.72	B5 V + B5 IV	2 (35)	n.e.	—	(24)
134481/2	κ^1/κ^2 Lup	3.87	B9.5 Vn + A3/5 V [28]	2 (35)	n.e.	—	
134505	ζ Lup	3.41	G8 III [44]	2 (35)	n.e.	—	
135379	β Cir	4.07	A3 IV [24]	2	n.e.	VAR	
135734	μ^1/μ^2 Lup	4.27	B7 V + B8 Ve [27,19]	2 (35)	n.e.	—	
136298	δ Lup	3.22	B1.5 IV [23]	2,9 (35,44)	BCEP	BCEP+SPB	(25)
136415/6	γ Cir	4.51	B5 IV + F8 V [23,47]	2 (18)	GCAS	VAR	
136504	ε Lup	3.37	B2 IV-V [23]	2,9 (35)	HB+SPB	HB+SPB	(11,14,62)
136664	ϕ^2 Lup	4.54	B4 V [23]	9 (44)	n.e.	—	
138690	γ Lup	2.78	B2 IV [23]	2,9 (35,44)	R	R	(77)
139127	ω Lup	4.33	K3 III [37]	2	n.e.	—	
139365	τ Lib	3.66	B2.5 V [23]	9 (44)	n.e.	HB+E	(44)
141556	χ Lup	3.95	B9.5 III [25]	9	n.e.	—	
142669	ρ Sco	3.88	B2 IV-V [23]	9 (44)	—	ELL	
143018	π Sco	2.89	B1 V + B2 [23]	9 (44)	ELL	E+BCEP	(17)
143118	η Lup	3.41	B2.5 IV [23]	9 (44)	CST:	VAR	
143275	δ Sco	2.32	B0.5 IV [23]	9 (44)	GCAS	VAR	
144217/8	β^1/β^2 Sco	2.62/4.69	B0.5 V + B2 V [1]	9 (44)	—	VAR	
144294	θ Lup	4.23	B2.5 Vn [23]	9 (44)	VAR:	—	(24)
144470	ω^1 Sco	3.96	B1 V [23]	9 (44)	n.e.	—	
145482	13 c^2 Sco	4.57	B3 Vn [24]	9	R+PULS	VAR	(24)
145502/1	ν Sco	4.01	B2 V + B9 Vp Si [48]	9 (44)	ACV	VAR	(24)
147165	σ Sco	2.89	B1 III [23]	9 (44)	BCEP	BCEP+SPB	(40)
148478/9	α Sco	0.96	M0.5 Iab + B3 V: [27]	9 (44)	SRC	VAR	
148688	V1058 Sco	5.39	B1 Ia [24]	9 (44)	ACYG	ACYG	
148703	N Sco	4.23	B2 III [23]	9 (44)	EA	E	(45)
149038	μ Nor	4.94	B0 Ia [23]	9 (44)	ACYG:	ACYG	(21)
149404	V918 Sco	5.47	O8.5 Iab(f)p [39]	9 (44)	ELL	ELL+ACYG	(54)
149438	τ Sco	2.81	B0 V [23]	9 (44)	n.e.	—	(14)
151680	ε Sco	2.29	K2.5 III [35]	9 (44)	—	VAR	(57)
151804	V973 Sco	5.22	O8 Ifp [23]	9 (44)	ACYG	ROT+ACYG	(50)
151890	μ^1 Sco	2.98	B1.5 IV + B [42]	9 (44)	EB/SD	E	
151985	μ^2 Sco	3.54	B2 IV [23]	9 (44)	n.e.	—	
157056	θ Oph	3.27	B2 IV [23]	3 (16,27,37,45,54,63)	BCEP+SPB	BCEP+SPB	(58)
157792	44 b Oph	4.17	A3m [45]	3 (16,27,37,45,54,63)	—	—	
157919	45 d Oph	4.29	F5 IV [38]	3 (16,27,37,45,54,63)	n.e.	—	
158408	υ Sco	2.69	B2 IV [23]	3 (16,27,37,45,54,63)	n.e.	VAR	
158926	λ Sco	1.63	B1.5 IV + B [42]	3 (16,27,37,45,54,63)	BCEP+EA	BCEP+E	
159433	Q Sco	4.29	K0 III [49]	3	—	—	
159532	θ Sco	1.86	F1 II [31]	3 (16,27,37,45,54,63)	—	VAR	
160578	κ Sco	2.41	B1.5 III [23]	3 (16,27,37,45,54,63)	BCEP	BCEP	
161471	ι^1 Sco	3.03	F2 Ia [2]	3 (16,27,37,45,54,63)	n.e.	—	
161592	3 (X) Sgr	4.54	F3 II [31]	3 (16,27,45)	DCEP	DCEP	(31,41)
161892	G Sco	3.21	K2 III [50]	3 (16,27,37,54)	n.e.	VAR	(57)

Table A.1: continued.

HD	Other designation	V (mag)	MK spectral type	BRITE field(s)	Variability class VSX	Variability class this paper	Notes, references to BRITE papers
164975	γ^1 (W) Sgr	4.69	F8p + A0 V [31,51]	3 (16,27,45,54)	DCEP	DCEP	(31,41)
165135	γ^2 Sgr	2.99	K1 III [50]	3 (16,27,37,54)	—	VAR	(57)
166937	μ Sgr	3.86	B8 Iap [6]	3 (16,27,37,45,54,63)	EA+ACYG	VAR	
167618	η Sgr	3.11	M3.5 III [35]	3 (16,27,45,54)	LB:	VAR	(57)
168454	δ Sgr	2.67	K3 III [42]	3 (16,27,37,45,54)	VAR:	—	
169022	ε Sgr	1.85	B9.5 III [42]	3 (16,27,37,45,54,63)	n.e.	—	
169916	λ Sgr	2.81	K0 IV [50]	3 (16,27,37,45,54)	n.e.	—	
173300	ϕ Sgr	3.17	B8 III [26]	3 (27,45)	n.e.	—	
186882	δ Cyg	2.87	B9.5 III [1]	4,10 (38)	CST	—	(76)
187849	19 (V1509) Cyg	5.12	M2 III [52]	4 (38,46)	LB	VAR	
188892	22 Cyg	4.94	B5 IV [10]	4,10 (38,46)	—	—	
188947	η Cyg	3.88	K0 III [13]	4 (17,64)	—	VAR	(57)
189178	—	5.45	B5 V [10]	10 (38)	n.e.	—	
189687	25 (V1746) Cyg	5.19	B2.5 V(e) [19]	4,10 (38,46,64)	GCAS+BCEP	BE	
189849	15 (NT) Vul	4.66	A4 IIIm: [8]	10 (17)	ACV	—	(34)
191610	28 (V1624) Cyg	4.93	B3 IVe [19]	4,10,(17,38,46,64)	SXARI+BE	BE+SPB	(36)
192577/8	31 (V695) Cyg	3.80	K2 II + B3 V [40]	4,10 (38,46)	EA/GS/D	VAR	
192640	29 (V1644) Cyg	4.97	A2 V [8]	4,10 (17,38,46,64)	DSCT	DSCT	
192685	QR Vul	4.78	B3 V [10]	10 (17,46)	GCAS	VAR	
192806	23 Vul	4.52	K3 III [13]	4	n.e.	VAR	(57)
192909/10	o^2 (V1488) Cyg	3.98	K3 Ib-II + B/A [40]	4 (38)	EA/GS/D	VAR	
193092	—	5.24	K4 II [13]	4 (64)	VAR	—	
193237	34 (P) Cyg	4.81	B1ep [10]	4,10 (17,38,46,64)	SDOR	SDOR	(13,78)
194093	γ Cyg	2.20	F5 II [2]	4,10 (38)	—	VAR	
194317	39 Cyg	4.43	K3 III [2]	4 (38)	n.e.	VAR	(57,73)
194335	V2119 Cyg	5.90	B2 IIIe [19]	10	BE	—	
195068/9	43 (V2121) Cyg	5.74	F2 V [16]	10 (29,38,46,64)	GDOR	GDOR	(29,32)
195295	41 Cyg	4.01	F5 II [2]	4,10 (46)	—	—	
195556	ω^1 (V2014) Cyg	4.94	B2.5 IV [10]	10 (38)	LERI:	VAR	
196093/4	47 (V2125) Cyg	4.66	K3 Ib + B7 [53]	4	LC	VAR	
197345	α Cyg	1.25	A2 Ia [2]	4,10 (17,38,46,64)	ACYG	VAR	
197912	52 Cyg	4.22	K0 III [13]	4	n.e.	—	
197989	ε Cyg	2.46	K0 III [13]	4,10 (46)	n.e.	—	(57)
198183	λ Cyg	4.53	B5 V [1]	4,10 (46,64)	GCAS	VAR	
198478	55 (V1661) Cyg	4.84	B3 Ia [2]	4,10 (29,64)	ACYG	ACYG	(21,46)
198639	56 Cyg	5.05	A6 V [16]	10 (29,64)	CST:	—	
198726	T Vul	5.77	F5 Ib [54]	4,10	DCEP	DCEP	(31,41)
198809	31 Vul	4.59	G5 III [54]	4	—	—	
199081	57 Cyg	4.78	B5 V [10]	4,10 (29,38,64)	—	VAR	
199629	ν Cyg	3.94	A1 Vn [8]	4,10 (38,64)	n.e.	—	
200120	59 (V832) Cyg	4.74	B1.5 Vnne [10]	4,10 (46,64)	GCAS+R	BE	
200310	60 (V1931) Cyg	5.37	B1 Vn [10]	10 (29,46,64)	LERI	BE	(26)
200905	ξ Cyg	3.72	K5 Ib [2]	4 (38,46,64)	LC	VAR	
201078	DT Cyg	5.82	F8 Ib-II [15]	4,10 (46)	DCEPS	DCEPS	(31,41)
201251	63 Cyg	4.55	K4 II [2]	4	—	—	
201433	V389 Cyg	5.69	B9 V [8]	10 (17)	SPB	SPB+E	(10,16)
202109	ζ Cyg	3.20	G8 II [2]	4,10 (46)	n.e.	—	
202444	τ Cyg	3.72	F0 IV [55]	4,10 (38)	DSCT	—	
202850	σ Cyg	4.23	B9 Ia [2]	4,10 (38,46)	ACYG	ACYG	(46)
202904	υ Cyg	4.43	B2 Ve [10]	4,10 (46)	GCAS	BE	
203064	68 (V1809) Cyg	5.00	O7.5 III((f))n [22]	4,10 (29,64)	ELL	—	
203156	V1334 Cyg	5.83	F1 II [15]	4,10	DCEPS	DCEPS	(31,41)
203280	α Cep	2.44	A7 IV/V [1]	11	DSCT	—	
205021	β Cep	3.23	B2 III [6]	11 (39)	BCEP	—	
205435	ρ Cyg	4.02	G8 III [13]	10 (38)	RS:	—	
206570	V460 Cyg (DS Peg)	6.07	C6,3 [56]	4	SRB	—	
207260	ν Cep	4.29	A2 Iae [25]	11	ACYG	VAR	
209790	ξ Cep	4.29	F7 V [48]	11	n.e.	—	

Table A.1: continued.

HD	Other designation	V (mag)	MK spectral type	BRITE field(s)	Variability class VSX	Variability class this paper	Notes, references to BRITE papers
209975	19 Cep	5.11	O9.5 Ib [2]	11 (57)	n.e.	ACYG	
210745	ζ Cep	3.35	K1 Ib [2]	11 (29,39)	LC	—	
211336	ε Cep	4.19	F0 IV [1]	11 (29,39,57)	DSCTC	DSCT	(28)
213306/7	δ Cep	3.75	F5 Ib + B8 V [57,48]	11 (29,39,57)	DCEP	DCEP	(31,41)
216228	ι Cep	3.52	K1 III [13]	11	n.e.	—	
218376	1 Cas	4.84	B0.5 IV [6]	11 (19,39,57)	n.e.	—	
220652	4 Cas	4.98	M2 III [58]	11 (39)	LB	VAR	
221253	AR Cas	4.88	B3 IV [10]	11 (19,39,57)	EA/DM	E	
224572	σ Cas	5.00	B1 V [10]	11 (19,39)	n.e.	—	
225289	V567 Cas	5.79	B8p HgMn [59]	11	ACV	—	

References. MK spectral types: [1] Johnson & Morgan (1953), [2] Morgan & Roman (1950), [3] Morgan & Keenan (1973), [4] Keenan & Pitts (1980), [5] Henry et al. (1994), [6] Morgan et al. (1955), [7] Cowley (1972), [8] Cowley et al. (1969), [9] Gray & Garrison (1989), [10] Lesh (1968), [11] Struve & Sahade (1957), [12] Keenan et al. (1987), [13] Roman (1952), [14] Walborn (1972), [15] Cowley (1976), [16] Abt & Morrell (1995), [17] Burnashev (1985), [18] Levato (1972), [19] Slettebak (1982), [20] Maíz Apellániz et al. (2018), [21] Conti & Alschuler (1971), [22] Sota et al. (2011), [23] Hiltner et al. (1969), [24] de Vaucouleurs (1957), [25] Gray & Garrison (1987), [26] Garrison & Gray (1994), [27] Corbally (1984), [28] Houk & Cowley (1975), [29] Ake & Parsons (1987), [30] Hiltner & Schild (1966), [31] Malaroda (1975), [32] Danks & Houziaux (1978), [33] Jaschek & Jaschek (1965), [34] Jaschek & Jaschek (1959), [35] Landi Dessy & Keenan (1966), [36] Parsons & Ake (1998), [37] Houk (1978), [38] Evans et al. (1957), [39] Sota et al. (2014), [40] Bidelman (1951), [41] Smith (1968), [42] Houk (1982), [43] Morris (1961), [44] Keenan & McNeil (1989), [45] Malaroda (1973), [46] Buscombe (1969), [47] Buscombe & Barkstrom (1971), [48] Slettebak (1963), [49] Wilson & Joy (1950), [50] Gray et al. (2006), [51] Evans (1991), [52] Bakos (1974), [53] Hendry (1981), [54] Nassau & van Albada (1947), [55] Slettebak (1955), [56] Keenan & Morgan (1941), [57] Kraft (1960), [58] Yamashita (1967), [59] Cowley (1968).
BRITE papers: (1) Weiss et al. (2016), (2) Pigulski et al. (2016), (3) Baade et al. (2016), (4) Moździerski & Pigulski (2016), (5) Buysschaert & Neiner (2016), (6) Handler et al. (2017b), (7) Daszyńska-Daszkiewicz et al. (2017a), (8) Pablo et al. (2017b), (9) Buysschaert et al. (2017b), (10) Kallinger et al. (2017), (11) Handler et al. (2017a), (12) Richardson et al. (2017b), (13) Richardson et al. (2017a), (14) Wade et al. (2017), (15) Buysschaert et al. (2017a), (16) Kallinger & Weiss (2017), (17) Pigulski et al. (2017), (18) Daszyńska-Daszkiewicz et al. (2017b), (19) Handler (2017), (20) Zocłońska (2017), (21) Rybicka (2017), (22) Pablo et al. (2017a), (23) Walczak et al. (2017), (24) Paunzen & Rode-Paunzen (2017), (25) Cugier & Pigulski (2017), (26) Baade et al. (2017), (27) Niemczura et al. (2017), (28) Zwintz (2017), (29) Gössl et al. (2017), (30) Kondrak et al. (2017), (31) Smolec et al. (2017), (32) Zwintz et al. (2017), (33) Ramiaramanantsoa et al. (2018a), (34) Smalley et al. (2018), (35) Krtička et al. (2018), (36) Baade et al. (2018a), (37) Mol Lous et al. (2018), (38) Moffat et al. (2018), (39) Baade et al. (2018c), (40) Pigulski et al. (2018a), (41) Smolec et al. (2018), (42) Zocłońska (2018), (43) Pablo et al. (2018), (44) Pigulski et al. (2018b), (45) Ratajczak & Pigulski (2018), (46) Rybicka et al. (2018), (47) Begy et al. (2018), (48) Zwintz (2018), (49) Kallinger & Weiss (2018), (50) Ramiaramanantsoa et al. (2018b), (51) Niemczura et al. (2018), (52) Krtička & Feldmeier (2018), (53) Baade et al. (2018b), (54) Rauw et al. (2019), (55) Buysschaert et al. (2019), (56) Schmutz & Koenigsberger (2019), (57) Kallinger et al. (2019), (58) Walczak et al. (2019), (59) Ratajczak et al. (2019), (60) Zwintz et al. (2019b), (61) Zwintz et al. (2019a), (62) Pablo et al. (2019), (63) Wade et al. (2020), (64) Borre et al. (2020a), (65) Oplištilová et al. (2020), (66) Krtička et al. (2020), (67) Jerzykiewicz et al. (2020), (68) Lovekin & Tompkins (2020), (69) Zwintz et al. (2020a), (70) Borre et al. (2020b), (71) Ramiaramanantsoa & Moffat (2020), (72) St-Louis et al. (2020), (73) Huber & Zwintz (2020), (74) Weiss et al. (2020), (75) Zwintz et al. (2020b), (76) Yeh & Jiang (2021), (77) Jerzykiewicz et al. (2021), (78) Elliott et al. (2022), (79) Oplištilová et al. (2023).

Appendix B: Notes on individual stars

In this appendix, we provide short notes on the BRITE-Constellation data from Fields 1 – 14 for each of the stars discussed in this paper, including interesting features appearing in the Fourier spectrum (FS). The objects are sorted by HD number. Information on additional observations in other BRITE fields and about variability, either known previously or found from BRITE data is included in Table A.1.

HD 432 (β Cas, Field 11): Known δ Scuti-type star. Clear variability is seen with a dominant signal at frequency 9.897 d^{-1} in the FS of the BAb, BLb, BHr and BTr data. The BRITE data are discussed in detail by Zwintz et al. (2020b).

HD 2905 (κ Cas, Field 11): The star is a B1 Ia-type supergiant observed by BAb, BHr and BLb, showing stochastic oscillations at low frequencies in the FS typical for evolved O and B stars (see, for example, Bowman et al. 2019).

HD 3360 (ζ Cas, Field 11): This is a β Cephei star for which the FS of the BLb data shows some weak variability with a frequency of 7.6715 d^{-1}. The FSa of the BAb and BTr data show multi-frequency variability at low amplitudes.

HD 3712 (α Cas, Field 11): No significant variability was detected in the BAb, BHr, BLb and BTr data.

HD 3901 (ξ Cas, Field 11): No significant variability was detected in the BAb data.

HD 4614 (η Cas, Field 11): No significant variability was detected in the BAb and BHr data.

HD 5394 (γ Cas, Field 11): This well-known Be star is also the prototype of a subclass of Be stars showing large-amplitude long-term variations. Clear variability detected in the BAb, BHr, BLb and BTr data. The BRITE data for this star are discussed in detail by Borre et al. (2020a).

HD 6811 (ϕ And, Field 11): No variability was detected in the BAb data.

HD 6961 (θ Cas, Field 11): No variability was detected in the BAb data.

HD 8538 (δ Cas, Field 11): No variability was detected in the BAb, BLb or BTr data.

HD 11415 (ε Cas, Field 11): Known Be star. Some low-frequency variability is present in the FS of the BAb data.

HD 16908 (35 Ari, Field 5): No variability was detected in the BAb data. The data set is short and scarce.

HD 17573 (41 Ari, Field 5): No variability was detected in the BAb data.

HD 17584 (16 Per, Field 5): Observed with UBr and BAb. The FS of the UBr data shows a frequency at ~4.9 d^{-1} or its alias at ~9.3 d^{-1} that can be attributed to δ Scuti-type pulsation. The BAb data set is short and scarce.

HD 17709 (17 Per, Field 5): No variability was detected in the UBr data. The data set is short and scarce.

HD 18296 (21 Per, Field 5): Observed with UBr and BAb. The FS of the UBr data reveals a dominant frequency of 0.343 d^{-1} (corresponding to a period of ~2.92 d). No variability was detected in the BAb data. Both data sets are short.

HD 19058 (ρ Per, Field 5): Observed with UBr. The light curve shows clear long-term variability.

HD 19356 (β Per, Algol, Field 5): Known eclipsing binary. Its variability with the 2.87-d period is clearly detectable in the UBr and BAb data.

HD 19373 (ι Per, Field 5): No variability was detected in the UBr data.

HD 19476 (κ Per, Field 5): No variability was detected in the UBr data.

HD 20365 (20 Per, Field 5): No variability was detected in the UBr data.

HD 20418 (31 Per, Field 5): No variability was detected in the UBr data.

HD 20468 (Field 5): No variability was detected in the UBr data.

HD 20809 (Field 5): Observed with UBr. The FS of the data reveals a signal at frequency 2.25 d^{-1}. The available data have a short time coverage.

HD 20902 (α Per, Field 5): No variability was detected in the UBr and BAb data.

HD 21428 (34 Per, Field 5): No variability was detected in the UBr data.

HD 21552 (σ Per, Field 5): Observed with UBr. The available data set is long and the FS of the data shows some moderate variability at low frequencies. This K3-type star was included in the study of Kallinger et al. (2019).

HD 22192 (ψ Per, Field 5): Known Be star, observed by UBr and BAb. The FS of the data reveals variability with a frequency of 0.986 d^{-1}.

HD 22780 (Field 5): No variability was detected in the UBr data.

HD 22928 (δ Per, Field 5): Observed by UBr and BAb. The FS of the UBr data shows clear variability with a frequency of ~1.27 d^{-1}, but additional peaks can also be identified. The BAb data are of lower quality, but their analysis confirms the frequency peaks identified from the UBr observations.

HD 23180 (o Per, Field 5): Observed with UBr and BAb. The FSa of the available data reveal clear variability with a frequency of 0.453 d^{-1}.

HD 23230 (ν Per, Field 5): No variability was detected in the BAb data.

HD 23302 (17 Tau, Field 5): No variability was detected in the BAb data. The FS of the UBr data shows only some weak variability at low frequencies.

HD 23338 (19 Tau, Field 5): No variability was detected in the UBr or BAb data.

HD 23408 (20 Tau, Field 5): Observed with UBr and BAb. Both data sets have long time bases. The FS reveals a significant peak at frequency of 0.965 d^{-1}. The light curve phased with the corresponding period does not show coherent variation, however.

HD 23480 (23 Tau, Field 5): No variability was detected in the UBr or BAb data.

HD 23630 (η Tau, Field 5): Known Be star, observed with UBr and BAb. The FSa show a single significant frequency at 0.03 d^{-1}.

HD 23850 (27 Tau, Field 5): Observed with UBr and BAb. The FS of the UBr data reveals three strong peaks at frequencies of ~0.41, ~0.82 and ~1.3 d^{-1}. The FS of the BAb data confirms the dominant frequency identified from the UBr observations.

HD 24398 (ζ Per, Field 5): Observed with UBr and BAb. The UBr light curve shows irregular variability resulting in several peaks in the low-frequency domain of the FS, the highest of which occurs at 0.04 d^{-1}. The BAb data confirm the character of the variability, which fits the ACYG classification.

HD 24640 (Field 5): No variability was detected in the BAb data.

HD 24760 (ε Per, Field 5): Observed with UBr and BAb. The FSa of the available data show multi-periodic hybrid β Cephei/SPB variability with the dominant peak at a frequency of 5.898 d^{-1}.

HD 24912 (ξ Per, Field 5): Observed with UBr and BAb. The FS of the UBr data shows clear variability with a frequency of

0.49 d^{-1}. The analysis of the BAb data confirmed the frequency detected based on the UBr observations.

HD 25823 (41 Tau, Field 5): Observed with UBr. The available data set is short, but its FS reveals variability with a frequency of 0.13 d^{-1}.

HD 25940 (48 Per, Field 5): Observed with UBr and BAb. The UBr data set is long and its FS shows variability with a frequency of ∼2.26 d^{-1}, which is confirmed with the shorter and scarcer BAb data set.

HD 25998 (50 Per, Field 5): No variability was detected in the UBr data.

HD 26322 (44 Tau, Field 5): Known δ Scuti star, observed with UBr. The δ Scuti variability is clearly present with the strongest peak in the FS at a frequency of 6.89 d^{-1}.

HD 26630 (μ Per, Field 5): No variability was detected in the UBr data.

HD 27396 (53 Per, Field 5): Observed with UBr. The FS of the available data shows multi-mode SPB-type variability with the strongest peak at a frequency of 0.46 d^{-1}.

HD 29248 (ν Eri, Fields 6 & 13): Known hybrid β Cephei/SPB star. *Field 6:* Observed with BAb, BTr, BHr and BLb. The available data clearly show the known β Cephei variability. *Field 13:* Observed with BAb and UBr. The available data also show the known pulsations. BRITE data for this star were discussed in detail by Handler et al. (2017b) in combination with ground-based observations.

HD 30211 (μ Eri, Fields 6 & 13): Known SPB star and eclipsing binary. *Field 6:* Observed with BTr, BHr, BLb and BAb. The strongest frequency in the FS is found at ∼0.61 d^{-1} for BTr, BHr, and BAb data and 0.69 d^{-1} for the BLb data, but the FSa show also the presence of many additional peaks. *Field 13:* Observed with UBr and BAb. The available data confirm the variability seen in the data from Field 6.

HD 30652 (π^3 Ori, Field 6): No variability was detected in the BTr data.

HD 30836 (π^4 Ori, Fields 6 & 13): Known spectroscopic binary. *Field 6:* Observed with BTr, BHr, BAb and BLb. The available data show clear variability with a period of ∼4.1 days. *Field 13:* Observed with BAb and UBr. The UBr data confirm the variability found from Field 6 data. The BAb data have a short time base and are scarce.

HD 31109 (ω Eri, Field 6). Known spectroscopic binary. Observed with BHr and BLb. The FSa of the available data show a dominant peak at a frequency of ∼3.64 d^{-1}, but the star is multiperiodic. The BLb light curve is shorter and noisier than that secured by BHr, but its analysis confirms the main frequency found from the BHr data.

HD 31139 (5 Ori, Field 6): Observed with BHr and BTr. Some long-term variability may be present in the BHr data, but the data are inconclusive. The BTr light curve is only ∼8 d long and does not reveal any variation.

HD 31237 (π^5 Ori, Fields 1, 6 & 13): Known ellipsoidal binary variable with an SPB component. *Field 1:* Observed with BAb and UBr. The available data clearly show the ellipsoidal variability with a period of 1.85 d. *Field 6:* Observed with BHr, BTr, BLb and BAb. The period of 1.85 d is again clearly visible. *Field 13:* Observed with UBr and BAb. The UBr data confirm the periodicity found from Field 1 and 6 data. The BAb data set is short and scarce. BRITE data are discussed in detail by Jerzykiewicz et al. (2020).

HD 31767 (π^6 Ori, Field 6): No clear variability was detected in the BTr data.

HD 33111 (β Eri, Fields 1 & 6): *Field 1:* Observed with BAb and UBr. Variability was detected in both data sets, although the strongest peaks in the FSa were found at different frequencies, 1.055 d^{-1} for the BAb data and 10.44 d^{-1} for the UBr data. *Field 6:* No variability was detected in the BTr data.

HD 33328 (λ Eri, Fields 6 & 13): Known Be star. *Field 6:* Observed with BAb, BHr, BTr and BLb. Variability detected in all data sets, although the strongest frequency peak is at ∼2.85 d^{-1} in the FS of the BHr data and at half of this frequency in the FSa of the BAb, BTr and BLb data. *Field 13:* No variability was detected in the BAb data. The available data have a short time base and are scarce.

HD 33904 (μ Lep, Field 6): No variability was detected in the BTr and BAb data. The BAb data set is scarce and of poor quality.

HD 34085 (β Ori, Rigel, Fields 1, 6 & 13): *Field 1:* Observed with BAb and UBr. The acquired CCD subraster of this star is severely overexposed resulting in low quality data. *Field 6:* Observed with BHr, BTr, BLb and BAb. The available data show some long-period variability. Due to the brightness of the star, the images were saturated and the origin of the variability may be partly instrumental. *Field 13:* Observed with UBr and BAb. The UBr data again show some long-period variability. The BAb data set is shorter and scarcer, but displays a similar behaviour to the UBr data set.

HD 34503 (τ Ori, Fields 1, 6 & 13): *Field 1:* No variability was detected in the BAb or UBr data. *Field 6:* No variability was detected in the BTr, BHr, BLb or BAb data. *Field 13:* No variability was detected in the BAb data. According to Pigulski et al. (2018b), the star shows a weak heartbeat signal.

HD 34816 (λ Lep, Field 6): Early B type star observed with BHr, BLb and BTr. The FS of the BHr data shows the strongest frequency peak at 5.79 d^{-1}. The BLb and BTr data are of lower quality and do not show any variability.

HD 35039 (22 Ori, Field 6): No variability was detected in the BTr data.

HD 35369 (29 Ori, Field 6): No variability was detected in the BTr data.

HD 35411 (η Ori, Fields 1, 6 & 13): Eclipsing binary star with an orbital period of 8 d. *Field 1:* Observed with BAb and UBr. Both data sets show eclipses and regular variability with a period of 0.432 d. *Field 6:* Observed with BTr, BHr, BLb and BAb. The data confirm the binary period and the additional regular variability. *Field 13:* Observed with UBr and BAb. Both data sets confirm the binary period and the additional variability.

HD 35439 (ψ^1 Ori, Field 6): Observed with BTr, BHr and BLb. The FSa of the available data show several distinct peaks in the g-mode range and additional variability typical for Be stars. The first broad assessment of the complex variability observed by BRITE-Constellation was given by Baade et al. (2018c).

HD 35468 (γ Ori, Fields 1, 6 & 13):*Field 1:* No variability was detected in the BAb and UBr data. *Field 6:* No variability was detected in the BTr, BHr, BLb and BAb data. *Field 13:* No variability was detected in the UBr and BAb data.

HD 35715 (ψ^2 Ori, Fields 1 & 6): *Field 1:* Observed with BAb and UBr. The available data show ellipsoidal variability with a period 2.526 d. *Field 6:* Observed with BTr, BHr, BLb and BAb. The data confirm the main period of 2.526 d. Pigulski et al. (2017) found in the BRITE data several additional frequencies attributable to p modes.

HD 36267 (32 Ori, Field 6): Observed with BTr, BHr and BLb. The data show variability with a period of 3.772 d.

HD 36485/6 (δ Ori, Fields 1, 6 & 13): Massive eclipsing and spectroscopic binary. *Field 1:* Observed with BAb and UBr. The data clearly show eclipses with an orbital period of 5.733 d and some additional variability. *Field 6:* Observed with BTr, BHr,

BLb and BAb. The data confirm the binary period. *Field 13:* Observed with UBr and BAb. The data confirm the binary period.

HD 36512 (υ Ori, Field 6): No variability was detected in the BTr, BHr or BLb data.

HD 36822 (ϕ^1 Ori, Field 6): No variability was detected in the BTr data.

HD 36861/2 (λ Ori A/B, Fields 1, 6 & 13): *Field 1:* No variability was detected in the BAb and UBr data. *Field 6:* No variability was detected in the BTr, BHr and BLb data. The BAb light cvurve is scarce and does not show any variability. *Field 13:* No variability was detected in the BAb data.

HD 36959/60 (Field 6): No variability was detected in BHr, BTr, BLb or BAb data.

HD 37018 (42 Ori, Field 6): No variability was detected in the BTr and BAb data.

HD 37022/41 (θ^1/θ^2 Ori, Fields 6 & 13): *Field 6:* Observed with BTr and BAb. The FS of the BTr data shows some marginal variability with a frequency of 0.62 d^{-1}. No variability was detected in the BAb data. *Field 13:* No variability was detected in the UBr data.

HD 37043 (ι Ori, Fields 1, 6 & 13): Known spectroscopic binary. *Field 1:* Observed with BAb and UBr. The FSa of the data show some variability in the low-frequency regime, but with no significant peaks. *Field 6:* Observed with BTr, BHr, BAb and BLb. The FSa of these data confirm variability in the low-frequency domain without a clear periodicity. *Field 13:* Observed with UBr and BAb. The FSa of the data confirm the variability in the low-frequency domain as seen from Field 1 and 6 data. BRITE data of this star were discussed by Pablo et al. (2017b).

HD 37128 (ε Ori, Fields 1, 6 & 13): B-type supergiant. *Field 1:* Observed with BAb and UBr. Both data sets show similar long-term variability, but no clear periodicity. This is characteristic for α Cyg-type variability. *Field 6:* Observed with BAb, BTr, BHr and BLb. The BAb data set is scarce and does show variability. The other data sets are of excellent quality and their FSa show clear and strong variability at low frequencies. *Field 13:* Observed with UBr and BAb. The FSa of these data clearly show variability in the low-frequency regime, but without a clear periodicity.

HD 37468 (σ Ori, Fields 1, 6 & 13): *Field 1:* Observed with BAb and UBr. The FS of the BAb data shows peak at a frequency of 0.84 d^{-1}. No variability was detected in the UBr data. *Field 6:* Observed with BAb, BLb, BHr and BTr. In the FSa of the BHr and BTr data, the strongest peak is located at a frequency of 1.68 d^{-1}, twice the frequency detected in the BAb data. In the FS of the BLb data the strongest peak lies again at frequency of 0.84 d^{-1}. The BAb data set is shorter and scarce. *Field 13:* Observed with UBr and BAb. The FS of the UBr data shows two peaks at 0.84 and 2.52 d^{-1}. No variability was detected in the BAb data, which are of lower quality.

HD 37490 (ω Ori, Fields 6 & 13): *Field 6:* Observed with BAb, BHr, BTr and BLb. The data show variability with the main period of about 0.95 d. *Field 13:* No variability was detected in the UBr data.

HD 37742/3 (ζ Ori A/B, Fields 1, 6 &13): O-type spectroscopic binary showing stochastic variability typical for massive stars (Buysschaert et al. 2017b). *Field 1:* Observed with BAb and UBr. The BAb light curve shows a period of 3.275 d. The corresponding frequency is not dominant in the FS of the UBr data, but a phase fold with the same period reveals similar variability. *Field 6:* Observed with BAb, BHr, BTr and BLb. The light curves show clear variability although the period of 3.275 d is not dominant in their FSa. *Field 13:* Observed with BAb and UBr. The FS of the UBr data clearly shows low-frequency variability. The BAb data are scarcer, but its FS confirms the variability at low frequencies.

HD 38771 (κ Ori, Fields 1, 6 & 13): B-type supergiant. *Field 1:* Observed with UBr and BAb. The FSa of the data show low-frequency signals with a dominating peak at a frequency of ~0.44 d^{-1}. *Field 6:* Observed with BHr, BLb, BTr and BAb. The FSa of the BHr and BLb data show clear variability with the strongest peak at a frequency of 0.9 d^{-1}. The BTr data set is shorter and its FS shows twice the frequency detected in the BHr and BLb data. The BAb data have a short time base and are scarce. *Field 13:* Observed with UBr and BAb. The FS of the UBr data shows variability in the low-frequency regime with a dominant peak at a frequency of 0.3016 d^{-1}. The BAb data are scarcer but its FS confirms the low-frequency variability.

HD 39060 (β Pic, Field 8): Young δ Scuti star, observed with BHr. The FS of the data reveals δ Scuti-type pulsations around 43 d^{-1}. Studied in detail by Zwintz et al. (2019b), Mol Lous et al. (2018) and Kenworthy et al. (2021).

HD 39801 (α Ori, Betelgeuse, Fields 1, 6 & 13): *Field 1:* Observed with BAb and UBr, but the acquired CCD subraster of this star was severely overexposed. *Field 6*: Observed with BAb, BTr, BHr and BLb. The data show clear variability, although part of this variability can be instrumental due to strong saturation (Weiss et al. 2021). The BAb data set is short and scarce. *Field 13:* Observed with UBr and BAb. The UBr data show some variability. No variability was detected in the scarce BAb data set.

HD 42933 (δ Pic, Field 8): Eclipsing binary, observed with BHr. The light curve clearly shows eclipses with a period of 1.672 d.

HD 44402 (ζ CMa, Field 12): Observed with BLb. The FS of the data shows a strong peak at a frequency of 0.2569 d^{-1}. The presence of additional frequencies is also evident.

HD 44743 (β CMa, Field 12): Known β Cep star. Observed with BTr and BLb. The FSa of the data show a clear peak at a frequency of 3.9791 d^{-1}.

HD 45348 (α Car, Field 8): No variability was detected in the BHr data.

HD 45871 (IY CMa, Field 12): Observed with BTr and BLb. The FS of the BTr data shows clear variability with the strongest peak at a frequency of 1.8503 d^{-1}, but additional frequencies can also be seen. The BLb data set is shorter, but confirms the variability detected from the BTr data.

HD 46328 (ξ^1 CMa, Field 12): Known magnetic β Cep-type pulsator. Observed with BHr, BTr and BLb. The FSa of the BTr and BLb data show clear variability with the strongest peak at a frequency of 4.7717 d^{-1}. The BHr light curve has two large gaps, but the frequency detected in the BLb and BTr data is confirmed. This star has been studied in detail using BRITE data by Wade et al. (2020).

HD 47306 (N Car, Field 8): No variability was detected in the BHr data.

HD 47670 (ν Pup, Field 8): Observed with BHr. The FS of the data displays a significant peak at a frequency of 0.6575 d^{-1}. The BRITE data were studied in detail by Baade et al. (2018a).

HD 48917 (10 CMa, Field 12): Known Be star, observed with BTr and BLb. The FS of the BTr data shows strong variability with the strongest peak at a frequency of 1.3364 d^{-1}. It is evident that several more frequencies are present. The BLb data have two large gaps but confirm the variability found from the BTr data.

HD 49131 (HP CMa, Field 12): No variability was detected in the BLb or BTr data.

HD 50013 (κ CMa, Field 12): Observed with BLb and BHr. FSa of both data sets show strong variability with a main peak at a frequency of 0.056 d^{-1}.

HD 50123 (HZ CMa, Field 12): Observed with BTr and BLb. The FS of the BTr data shows a frequency of 0.07 d^{-1}, which corresponds to twice the frequency of the known ellipsoidal variability (Sterken et al. 1994). The BLb data set is shorter, but confirms this variability.

HD 50337 (V415 Car, Field 8): No variability was detected in the BHr data.

HD 50707 (15 CMa, Field 12): Observed with BTr, BHr and BLb. The FSa of the data show clear β Cep-type pulsations with the strongest peak at a frequency of 5.418 d^{-1}.

HD 50877 (o^1 CMa, Field 12): Observed with BHr. The light curve shows strong long-term variability.

HD 50896 (EZ CMa, Field 12): Observed with BHr. The data show rotational modulation with a period of 3.656 d. They are discussed by Schmutz & Koenigsberger (2019).

HD 51309 (ι CMa, Field 12): Observed with BTr, BHr and BLb. The FSa of the data show variability with the strongest peak at a frequency of 0.077 d^{-1}, but additional frequencies that can be attributed to β Cep pulsations are evident.

HD 52089 (ε CMa, Field 12): No variability was detected in the BHr or BLb data.

HD 52670 (LS CMa, Field 12): Observed with BTr. The data show three eclipses, two primary and one secondary.

HD 52877 (σ CMa, Field 12): Observed with BHr. The data show strong long-term variability with a period of about 34 d.

HD 53138 (o^2 CMa, Field 12): Blue supergiant, observed with BHr and BLb. The FSa of the data reveal strong variability with low frequencies.

HD 53244 (γ CMa, Field 12): No variability was detected in the BTr data.

HD 54309 (FV CMa, Field 12): No variability was detected in the BLb data.

HD 54605 (δ CMa, Field 12): No variability was detected in the BHr or BLb data.

HD 55892 (QW Pup, Field 8): Observed with BHr. The FS of the data shows multi-periodic γ Dor-type pulsations with a dominant frequency of 0.975 d^{-1}.

HD 56014 (27 CMa, Field 12): Observed with BLb, BHr and BTr. The FSa of the data reveal multi-periodic variability with the strongest peak at a frequency of 0.7925 d^{-1} for this Be star. The BLb light curve is of lower quality, but confirms the variability seen in the other light curves.

HD 56022 (OU Pup, Field 8): No variability was detected in the BHr data.

HD 56139 (ω CMa, Field 12): Observed with BHr, BTr and BLb. The data show strong variability, typical for Be stars.

HD 56455 (PR Pup, Field 8): Observed with BHr. The data are scarce, but its FS shows a significant frequency at 0.484 d^{-1}.

HD 56855 (π Pup, Field 8): No variability was detected in the BHr data.

HD 57060 (29 CMa, Field 12): Observed with BHr, BLb and BTr. All data sets show clear eclipses with a period of about 4.4 d.

HD 57061 (τ CMa, Field 12): Observed with BTr, BHr and BLb. The FSa of the data are dominated by a frequency of 1.56 d^{-1}, corresponding to twice the orbital frequency of the known variability due to eclipses (van Leeuwen & van Genderen 1997).

HD 58155 (NO CMa, Field 12): Observed with BTr and BLb. The BTr data reveal variability with a main period of 0.4774 d. The BLb data set is shorter and scarce.

HD 58286 (Field 12): No variability was detected in the BLb data.

HD 58343 (FW CMa, Field 12): Observed with BTr and BLb. The FS of the BTr data shows variability with the strongest peak at a frequency of 0.0772 d^{-1}. The BLb data set is shorter and scarce.

HD 58350 (η CMa, Field 12): Blue supergiant, observed with BHr and BLb. The FS of the data shows strong low-frequency variability with the strongest peak at 0.1222 d^{-1}.

HD 61068 (PT Pup, Field 12): Observed with BLb and BTr. The FSa of the data show β Cep-type variability with the strongest peak at a frequency of 5.9977 d^{-1}, see Handler (2017).

HD 61715 (MY Pup, Field 8): Known classical Cepheid. Observed with BHr. The data show clear variability with a period of about 5.7 d.

HD 62623 (3 Pup, Field 12): Observed with BHr and BLb. The FSa of the data show low-frequency variability typical for α Cyg-type stars.

HD 62747 (V390 Pup, Field 12): Known binary system, observed with BTr. The data show shallow eclipses with an orbital period of about 3.93 d.

HD 63462 (o Pup, Field 12): Observed with BTr, BHr and BLb. The FSa of all data sets show some low-frequency variability around 0.05 d^{-1}.

HD 63744 (Q Pup, Field 7): No variability was detected in the BTr data.

HD 63922 (P Pup, Fields 7 & 8): *Field 7:* No variability was detected in the BAb or BTr data. *Field 8:* No variability was detected in the scarce BHr data set.

HD 63949 (QS Pup, Field 8): No variability was detected in the BHr data.

HD 64440 (a Pup, Fields 7 & 8): *Field 7:* Observed with BAb and BTr. The FS of the BTr data shows a significant peak at ~1.9 d^{-1}. No variability was detected in the scarce BAb data set. *Field 8:* No variability was detected in the BHr data.

HD 64740 (Fields 7, 8 & 14): *Field 7:* Observed with BAb and BTr. The FSa of the data show a clear peak at a frequency of 0.7519 d^{-1}. In addition, the FS of the BTr data shows the presence of additional frequencies up to 2 d^{-1}. *Field 8:* No variability was detected in the scarce BHr data set. *Field 14:* No variability was detected in the short and scarce BAb data set.

HD 64760 (J Pup, Fields 7, 8 & 14): *Field 7:* Observed with BAb and BTr. The data show some indications for low-frequency variability in the FS. *Field 8:* No variability was detected in the scarce BHr data. *Field 14:* No variability was detected in the short and scarce BAb data.

HD 65575 (χ Car, Fields 7, 8 & 14): *Field 7:* Observed with BTr and BAb. The FS of the BTr and BAb data show multi-periodic variability with the strongest peaks at frequencies of 0.6438 d^{-1} and 0.6126 d^{-1}, respectively. *Field 8:* Observed with BHr. The light curve is scarce, but its FS shows variability with a frequency of 0.66 d^{-1}. *Field 14:* No variability was detected in the short and scarce BAb data set.

HD 65818 (V Pup, Fields 7, 8 & 14): Known eclipsing binary consisting of two B-type stars. *Field 7:* Observed with BTr and BAb. The data clearly show eclipses with the orbital period of about 1.45 d. *Field 8*: Observed with BHr. The data set is relatively short, but the variability is clearly detectable. *Field 14:* Observed with BAb. Again, the data set is relatively short, but confirms the period found from the other BRITE observations.

HD 66811 (ζ Pup, Fields 7, 8 & 14): O-type supergiant. *Field 7:* Observed with BTr and BAb. The FSa of the data show clear variability with a frequency of 0.562 d^{-1}. *Field 8:* Observed with BHr. The FS of the data shows the same frequency as detected

in the Field 7 data set. *Field 14:* No variability was detected in the short and scarce BAb data. The star was studied in detail by Ramiaramanantsoa et al. (2018a).

HD 67523 (ρ Pup, Field 12): Known δ Sct star observed with BLb, BHr and BTr. The FSa of the data show the variability with the strongest peak at a frequency of 7.098 d^{-1}.

HD 68243/73 (γ^1/γ^2 Vel, Fields 7, 8 & 14): Wolf-Rayet star. *Field 7:* Observed with BTr and BAb. The FSa of the data clearly show low-frequency variability. *Field 8:* Observed with BHr. The FS of the data confirms the low-frequency variability. *Field 14:* No variability was detected in the short and scarce BAb data set. Using BRITE-Constellation data, γ Vel was studied in detail by Richardson et al. (2017b).

HD 68553 (h^1 Pup, Field 7): Observed with BTr. The data show clear variability.

HD 69142 (h^2 Pup, Field 7): No variability was detected in the short and scarce BTr data set.

HD 71129 (ε Car, Field 7): Observed with BAb and BTr. The BAb data set is short, and its FS shows variability with the strongest frequency at 1.1289 d^{-1}. The BTr light curve confirms this variability.

HD 72127 (Field 7): No variability was detected in the short and scarce BAb data set.

HD 73634 (e Vel, Field 7): No variability was detected in the BTr and short and scarce BAb data sets.

HD 74006 (β Pyx, Field 7): No variability was detected in the BTr data and in the short and scarce BAb data set. The star was included in the study by Kallinger et al. (2019).

HD 74180 (b Vel, Field 7): No variability was detected in the BAb and BTr data.

HD 74195 (o Vel, Fields 7 & 14): *Field 7:* Observed with BAb and BTr. The FSa of the data show pulsations with a main frequency of 0.3574 d^{-1}. *Field 14:* Observed with BAb. The data set is relatively short and scarce, but its FS reveals variability with a frequency of 0.3597 d^{-1}.

HD 74375 (d Car, Field 7): Observed with BAb and BTr. The FSa of the data show clear pulsational variability with the strongest peak at a frequency of 0.4202 d^{-1}.

HD 74560 (HY Vel, Field 7): Observed with BAb. The data set is short and scarce, but its FS shows variability with a frequency of 0.63 d^{-1}.

HD 74575 (α Pyx, Field 7): Observed with BAb and BTr. The FSa of the data clearly show multi-periodic variability with the strongest peak at a frequency of 0.1876 d^{-1}.

HD 74772 (d Vel, Field 7): No variability was detected in the BTr data and short and scarce BAb data set.

HD 74956 (δ Vel, Field 7): Known eclipsing binary, observed with BAb and BTr. The light curves show eclipses with the orbital period of 45.15 d.

HD 75063 (a Vel, Field 7): Observed with BTr and BAb. The BTr data set is short and shows weak variability. No variability was detected in the short and scarce BAb data set.

HD 75311 (f Car, Fields 7 & 14): Known Be star. *Field 7:* Observed with BTr. The FS of the data reveals complex variability, with multiple intrinsic frequencies. *Field 14:* No variability was detected in the short and scarce BAb data set.

HD 75821 (f Vel, Field 7): No variability was detected in the short and scarce BAb data set.

HD 76728 (c Car, Fields 7 & 14): *Field 7:* Observed with BTr and BAb. The FS of the BTr data shows variability with a frequency of 0.293 d^{-1}. No variability was detected in the BAb data. *Field 14:* No variability was detected in the short and scarce BAb data set.

HD 77002 (b^1 Car, Field 7): No variability was detected in the short and scarce BTr data set.

HD 78004 (c Vel, Field 7): No variability was detected in the BTr data set. The BAb data set consists only of a few data points.

HD 78647 (λ Vel, Field 7): Observed with BTr and BAb. The BTr light curve shows complex long-term variability. The BAb data set is short and scarce.

HD 79351 (a Car, Fields 7 & 14): *Field 7:* Observed with BTr and BAb. The FS of the BTr data shows multi-frequency variability with the strongest peak at a frequency of 0.3725 d^{-1}. The FS of the BAb data confirms the multi-frequency variations, but the data are noisier. *Field 14:* No variability was detected in the short and scarce BAb data set.

HD 79940 (k Vel, Field 7): No variability was detected in the short and scarce BTr data.

HD 80230 (g Car, Field 7): Observed with BTr. The light curve shows a dominant period of 12.17 d.

HD 80404 (ι Car, Fields 7 & 14): *Field 7:* No variability was detected in the BTr and BAb data. *Field 14:* Observed with BAb. The data set is short and scarce, but its FS shows variability with a frequency of 1.1509 d^{-1}.

HD 81188 (κ Vel, Fields 7 & 14): *Field 7:* Observed with BTr and BAb. The FS of the data shows multi-frequency variability with the strongest peak at a frequency of 0.2431 d^{-1}. *Field 14:* No variability was detected in the short and scarce BAb data set.

HD 82434 (ψ Vel, Field 7): No variability was detected in the BTr data and the short and scarce BAb data set.

HD 82668 (N Vel, Field 7): Observed with BTr and BAb. The FS of the BTr data shows complex multi-frequency variability, while the BAb data set is short and scarce.

HD 83183 (h Car, Field 7): No variability was detected in the BTr data and in the short and scarce BAb data set.

HD 83446 (M Vel, Field 7): Observed with BTr and BAb. The FS of the BTr data show δ Sct-type variability with the strongest peak at a frequency of 31.08 d^{-1}. The BAb data set is shorter and of inferior quality.

HD 86440 (ϕ Vel, Field 7): No variability was detected in the BAb and BTr data.

HD 118716 (ε Cen, Field 2): Known β Cep star, observed with BTr, BLb, UBr and BAb. The FSa of the UBr and BAb data show clear pulsational variability with many frequencies and the strongest peak at a frequency of 5.8955 d^{-1}. The BTr and BLb data sets are scarce, but the main pulsation frequency can still be identified in the FSa of both data sets.

HD 120307 (ν Cen, Field 2): Observed by BTr, BLb, BAb and UBr. The BAb and UBr data are of excellent quality and show clear variability with a period of about 2.62 d. The BTr and BLb data sets are significantly shorter, but confirm the variability. The variability is due to the reflection effect in a binary system (Jerzykiewicz et al. 2021).

HD 120324 (μ Cen, Field 2): Known Be star, observed by BLb, BTr, BAb and UBr. The BAb and UBr data show significant, possibly irregular variations. The BLb and BTr data sets are shorter, but confirm the variability. BRITE data of this star were studied in detail by Baade et al. (2016).

HD 121263 (ζ Cen, Field 2): Heartbeat binary star observed with BAb, UBr, BLb and BTr. In the FSa of the BAb and UBr data the strongest peaks lie at a frequency of 0.1244 d^{-1}, corresponding to a period of ~8.026 d. The data sets from BLb and BTr are shorter, but confirm the detected period.

HD 121743 (ϕ Cen, Field 2): Observed with UBr, BTr, BAb and BLb. The FSa of the BAb and BLb data show the strongest peak at a frequency of 0.88 d^{-1}. This signal is weaker in the FSa of the UBr and BTr data, however.

HD 121790 (υ^2 Cen, Field 2): No variability was detected in the BAb data or UBr data sets. The BAb observations have a large gap in the middle of the run. The BTr data set is short and scarce.

HD 122451 (β Cen, Field 2): Observed with BAb, UBr, BTr and BLb. As this star is very bright, the acquired CCD subraster was overexposed and parts of the light curves have high scatter. The FS of the BAb data shows multi-frequency pulsations with the strongest peak at a frequency of 0.8689 d^{-1}. The UBr data are of similar quality. The BTr and BLb data sets are shorter.

HD 122980 (χ Cen, Field 2): Observed with BAb, UBr and BTr. The BAb data set has a gap in the centre and does not show any significant variability. The FS of the UBr data shows the strongest peak at ~1.002 d^{-1}, which is of instrumental origin. The BTr data set is significantly shorter and does not show any variability.

HD 125238 (ι Lup, Field 2): Observed with UBr, BAb and BTr. The UBr data set has the longest time base and best quality and its FS shows several peaks in the low frequency domain; the strongest peak is located at a frequency of 0.2974 d^{-1}. The BAb data set has a gap in the centre and the BTr data set has a significantly shorter time base. The FSa of both data sets confirm the low-frequency variability detected in the UBr data.

HD 125823 (a Cen, Field 2): Observed with UBr, BTr and BAb. The UBr light curve reveals rotational variability with a period of ~8.85 d. The BAb light curve has a gap in the centre, but confirms the period obtained with the UBr data. The BTr light curve is significantly shorter, but the variability is consistent with that seen in the UBr and BAb light curves.

HD 126341 (τ^1 Lup, Field 2): Known β Cep-type pulsator, observed with BAb, UBr, BTr and BLb. The FSa of the BAb and UBr data show the strongest peak at frequency of ~5.6 d^{-1}. The BTr and BLb data have shorter time bases, but confirm this variability.

HD 126354 (τ^2 Lup, Field 2): Observed with UBr, BAb and BTr. The FS of the UBr data shows an instrumental frequency of about 1 d^{-1} and a few lower-amplitude peaks. The BAb data set has a gap in the middle and the BTr data set has shorter time base, but their FSa confirm the frequencies found from the UBr data set.

HD 127381 (σ Lup, Field 2): Observed with UBr, BAb and BTr. The FS of the UBr data shows a clear peak at a frequency of 0.33 d^{-1}. The BAb data set has a gap in the middle of the run. The BTr data set is significantly shorter, but both data sets confirm the variability detected from the UBr observations.

HD 127972/3 (η Cen, Field 2): Known Be star, observed with BTr, BLb, UBr and BAb. The FSa of the UBr and BAb data show clear variability with the strongest peak at a frequency of 1.55 d^{-1}. The BTr and BLb data sets are shorter, but their analysis confirmed the main frequency found from the UBr and BAb data. BRITE data of this star were studied in detail by Baade et al. (2016).

HD 128345 (ρ Lup, Field 2): Observed with UBr, BAb and BTr. The FS of the UBr data shows clear variability with a frequency of 2.245 d^{-1}. The BAb data set has a gap in the middle of the run, but its analysis confirms this variability. The BTr data set is shorter and of poorer quality.

HD 128620/1 (α Cen, Field 2): Observed with BAb, BTr and BLb. The BAb light curve shows a period of 29.85 d. The BTr and BLb data sets are shorter and of poorer quality. Due to the brightness of the star, the acquired CCD subraster is severely overexposed and parts of the light curves have increased scatter.

HD 128898 (α Cir, Field 2): Known roAp star. Observed with BAb, UBr, BLb and BTr. The FS of the BAb data has the strongest peak at 0.225 d^{-1}. The strongest peak in the FS of the UBr data is located at the harmonic of this frequency. The roAp pulsations are also clearly detectable in the UBr and BAb data sets. The BLb and BTr data sets are shorter, but theis FSa confirm the strongest peak found from the BAb data and the roAp pulsations. All available BRITE data of this star were analysed by Weiss et al. (2016) and Weiss et al. (2020).

HD 129056 (α Lup, Field 2): Known β Cep-type star. Observed with BAb, UBr, BTr and BLb. The β Cep variability is seen in the FSa of the BAb and UBr data with the main peak at a frequency of 3.8487 d^{-1} and several smaller peaks at other frequencies. The BTr and BLb data sets are shorter, but their FSa confirm the strongest peak found in the analysis of the BAb and UBr data sets.

HD 129116 (b Cen, Field 2): No variability was detected in the UBr, BAb, and BTr data.

HD 130807 (o Lup, Field 2): Observed with UBr, BAb and BTr. The FS of the UBr data shows several significant frequencies with the strongest peak at a frequency of 1.106 d^{-1}. The BAb data set has a gap in the middle of the run and the BTr data set is significantly shorter, but FSa of both confirm the strongest frequency found in the FS of the UBr data. The variability of this magnetic star was described by Buysschaert et al. (2019).

HD 132058 (β Lup, Field 2): Observed with UBr, BAb, BTr and BLb. The UBr and BAb data show variability with a main period of 3.632 d. The BTr and BLb data have significantly shorter time bases, but confirm the main period obtained from the UBr and BAb data.

HD 132200 (κ Cen, Field 2): Observed with UBr, BAb, BTr and BLb. The FSa of the UBr and BAb data show multiple significant frequencies around ~0.698 d^{-1}. The BTr and BLb data sets are significantly shorter, but their analysis confirms this variability.

HD 133242/3 (π Lup, Field 2): No variability was detected in the BTr data.

HD 134481/2 (κ Lup, Field 2): No variability was detected in the UBr, BAb and BTr data. The BAb data set has a gap in the middle of the run and the BTr data set is rather short.

HD 134505 (ζ Lup, Field 2): No variability was detected in the UBr, BAb, BTr and BLb data. The BTr and BLb data sets are short.

HD 135379 (β Cir, Field 2): Observed with UBr, BAb and BTr. The FSa of the UBr and BAb data show low-frequency variability. The BAb data set has a gap in the middle of the run and the BTr data have a relatively short time base.

HD 135734 (μ Lup, Field 2): No variability was detected in the UBr, BAb and BTr data. The BTr data set is short.

HD 136298 (δ Lup, Fields 2 & 9): *Field 2:* Observed with UBr, BAb, BTr and BLb. The FSa of the UBr and BAb data show several significant frequencies in the domain of SPB stars, with the strongest peak at ~1.27 d^{-1}. The BTr and BLb data sets are significantly shorter, but their FSa confirm the strongest peak discovered from the UBr and BAb observations. *Field 9:* Observed with BAb, BLb, BHr and UBr. The FSa of the data show a clear signal at 5.902 d^{-1} as well as many other frequencies. The BRITE data for this star were discussed by Cugier & Pigulski (2017).

HD 136415/6 (γ Cir, Field 2): Observed with UBr, BAb and BTr. The FS of the UBr data shows a few significant frequencies, the strongest signal at 2.46 d^{-1} and the second strongest at 4.49 d^{-1}. The BAb data set has a large gap in the middle of the run and does not show any variability. The BTr data set is significantly shorter, but its FS confirms the two strongest peaks found in the FS of the UBr data.

HD 136504 (ε Lup, Fields 2 & 9): *Field 2*: Observed with UBr, BAb, and BTr. The UBr light curve shows a clear period of ∼4.55 d; some smaller peaks in the FS of the UBr data might also be intrinsic. The BAb data set has a gap in the middle of the run, but confirms the main period found from the UBr observations. The BTr data set is too short for any conclusive analysis. *Field 9*: Observed by BLb. The BLb light curve was analysed by Pablo et al. (2019), who identified a weak intrinsic signal at the orbital frequency. The light curve is otherwise free of any obvious variability.

HD 136664 (ϕ^2 Lup, Field 9): No variability was detected in the noisy BHr data set.

HD 138690 (γ Lup, Fields 2 & 9): Close visual double, one component of which is a single-lined spectroscopic system with an orbital period of 2.8 d. *Field 2:* Observed with UBr, BAb, BTr and BLb. The UBr and BAb data show clear variability with the orbital period. The BTr and BLb data sets are significantly shorter, but the same variability can also be identified. *Field 9:* Observed with BLb, UBr, BHr and BAb. The FSa of the BLb, UBr and BHr data show a clear peak at 0.351 d^{-1}, corresponding to the orbital period. The BAb data set is short and scarce. A detailed analysis of the BRITE data of this star was presented by Jerzykiewicz et al. (2021).

HD 139127 (ω Lup, Field 2): No variability was detected in the short (8 days long) UBr data set.

HD 139365 (τ Lib, Field 9): Early B-type spectroscopic binary exhibiting a heartbeat. Observed with BHr, UBr and BLb. The data show variability with the orbital period of 3.45 d. These results were first reported by Pigulski et al. (2018b).

HD 141556 (χ Lup, Field 9): No variability was detected in the BLb, BHr or UBr data.

HD 142669 (ρ Sco, Field 9): Observed with BLb, UBr and BHr. The BLb light curve exhibits small scatter and its FS reveals a highly significant signal at 0.3697 d^{-1}. This frequency is also found in the FS of the BHr data. The UBr data are of inferior quality and show no significant signal. When phased according to the corresponding period, the BLb and BHr data yield a light curve that is consistent with ellipsoidal variability.

HD 143018 (π Sco, Field 9): Observed with BAb, BHr, BLb and UBr. The FSa of the data show clear variability with the most prominent frequency at 1.2735 d^{-1} which is twice the orbital frequency. The data were analysed in detail by Pigulski et al. (2017), who found also pulsation with a frequency corresponding to a *p* mode.

HD 143118 (η Lup, Field 9): Observed with BLb, UBr and BHr. The FS of the BLb data shows a weak signal at 0.206 d^{-1}. No signal was detected in the noisier UBr and the shorter BHr data sets.

HD 143275 (δ Sco, Field 9): This is an early B-type Be star in an extraordinarily eccentric, 10.8-yr spectroscopic binary. Observed by BLb, UBr and BAb. The FSa of the data show a weak low-frequency variation.

HD 144217/8 (β^1 /β^2 Sco, Field 9): Observed with UBr, BLb and BAb. The FSa of the UBr and BLb data show a signal at 0.448 d^{-1} with a possible triplet structure. The BAb data set is sparse.

HD 144294 (θ Lup, Field 9): No variability was detected in the BLb data.

HD 144470 (ω^1 Sco, Field 9): No variability was detected in the BLb, BHr, UBr and BAb data.

HD 145482 (c^2 Sco, Field 9): Observed with BHr. The FS of the data shows clear signals at 0.173 d^{-1} and 1.177 d^{-1}.

HD 145502/1 (ν Sco, Field 9): Observed with UBr and BLb. The FS of the UBr data shows a clear signal at 0.172 d^{-1} and possible additional peaks at 0.824 d^{-1} and 1.174 d^{-1} with a possible triplet centred at 1.574 d^{-1}. The BLb data set is of insufficient length to reveal the signal.

HD 147165 (σ Sco, Field 9): This is a binary system consisting of two early B-type main-sequence components, with the primary star exhibiting β Cep-type pulsations. Observed by BHr, BLb, UBr and BAb. The FSa of the data show complex variability with a principal peak at 4.0509 d^{-1}, but with several other peaks of comparable amplitude. The BRITE observations were first discussed and interpreted by Pigulski et al. (2018a).

HD 148478/9 (α Sco, Antares, Field 9): M-type supergiant, observed by UBr, BLb and BAb. The light curves show long-term variability.

HD 148688 (V1058 Sco, Field 9): Early B-type supergiant, observed by BHr. The FS of the data shows stochastic low-frequency variability typical for evolved B-type stars.

HD 148703 (N Sco, Field 9): Eccentric eclipsing binary system observed by BHr, UBr and BLb. The BHr and UBr light curves reveal eclipses. The orbital period of the system is long and the BLb light curve does not cover any eclipse.

HD 149038 (μ Nor, Field 9): Observed with BHr. The FS of the data shows the typical stochastic low-frequency signal characteristic of evolved O and B-type stars.

HD 149404 (V918 Sco, Field 9): Evolved, post-Roche-lobe overflow non-eclipsing O-type binary, observed with BHr. The FS appears as typical for an O-type supergiant with a strong peak at 0.205 d^{-1} corresponding to half the 9.84-d orbital period. A detailed study of the BHr data (in combination with the SMEI data) was presented by Rauw et al. (2019).

HD 149438 (τ Sco, Field 9): No variability was detected in the UBr, BHr and BLb data. The BLb measurements show some minor contamination due to scattered moonlight near dates of lunar conjunction.

HD 151680 (ε Sco, Field 9): No variability was detected in the BLb and UBr data.

HD 151804 (V973 Sco, Field 9): Observed with BHr. The FS of the data exhibits a typical stochastic low-frequency signal of evolved O-type stars.

HD 151890 (μ^1 Sco, Field 9): Observed with UBr, BHr and BLb. The FSa of the data show strong variability with a frequency of 1.383 d^{-1}, corresponding to half of the known 1.446 d orbital period.

HD 151985 (μ^2 Sco, Field 9): Observed with BLb, BHr and UBr. The FSa of the BLb and BHr data show a weak signal at 1.383 d^{-1}, the same as detected in the nearby (5.8′ apart) μ^1 Sco. This means that the photometry pipeline did not separate well the contribution from both stars. The FS of the UBr data shows a somewhat weaker signal at this frequency, but also at twice this value which is 2.765 d^{-1}.

HD 157056 (θ Oph, Field 3): This well known β Cephei star was observed by UBr. The data set is short and scarce, but its FS reveals the most prominent pulsation frequency of 7.118 d^{-1}. This star was studied in detail using BRITE data by Walczak et al. (2019).

HD 157792 (b Oph, Field 3): Observed by UBr. No variability was detected in the short and scarce UBr data set.

HD 157919 (d Oph, Field 3): Observed by UBr. No variability was detected in the short and scarce UBr data set.

HD 158408 (υ Sco, Field 3): Observed with UBr. The data set is short and scarce, but the light curve shows signal with a period of 2.47 d.

HD 158926 (λ Sco, Field 3): The star is known to be an eclipsing β Cep star. Observed with UBr. The data set is short

and scarce and its FS shows a high amplitude peak at a frequency of 4.679 d^{-1}.

HD 159433 (Q Sco, Field 3): No variability was detected in the short and scarce UBr data set.

HD 159532 (θ Sco, Field 3): Observed with UBr. The data set is short and scarce and shows a period of ∼13 d.

HD 160578 (κ Sco, Field 3): Known β Cep-type star. Observed with UBr. The data set is short and scarce and its FS shows a high amplitude peak at a frequency of 5.001 d^{-1}.

HD 161471 (ι^1 Sco, Field 3): No variability was detected in the short and scarce UBr data set.

HD 161592 (X Sgr, Field 3): Classical Cepheid, observed with UBr. The data set is short and scarce but clearly shows the variability with the known period of 7.1 d.

HD 161892 (G Sco, Field 3): No variability was detected in the short and scarce UBr data set. The star was included in the study of Kallinger et al. (2019).

HD 164975 (γ^1 Sgr, Field 3): Classical Cepheid, observed with UBr. The data set is short and scarce, but clearly shows variability with a period of 7.7 d.

HD 165135 (γ^2 Sgr, Field 3): No variability was detected in the short and scarce UBr data set. The star was included in the study of Kallinger et al. (2019).

HD 166937 (μ Sgr, Field 3): Observed with UBr. The data set is short and scarce with some indication of variability.

HD 167618 (η Sgr, Field 3): Observed with UBr. The light curve is short and scarce and shows an irregular long-term variability.

HD 168454 (δ Sgr, Field 3): No variability was detected in the short and scarce UBr data set.

HD 169022 (ε Sgr, Field 3): No variability was detected in the short and scarce UBr data set.

HD 169916 (λ Sgr, Field 3): No variability was detected in the short and scarce UBr data set.

HD 173300 (ϕ Sgr, Field 3): No variability was detected in the short and scarce UBr data set.

HD 186882 (δ Cyg, Fields 4 & 10): *Field 4:* No variability was detected in the BLb, UBr and BTr data sets. *Field 10:* No variability was detected in the BAb, BLb and UBr data.

HD 187849 (19 Cyg, Field 4): Observed with BTr. The data set is relatively short and shows strong and clear variability with a period of ∼28.4 d.

HD 188892 (22 Cyg, Fields 4 & 10): *Field 4:* No variability was detected in the short and scarce BLb data set. *Field 10:* No variability was detected in the BTr and UBr data.

HD 188947 (η Cyg, Field 4): No variability was detected in the BTr, UBr and BLb data. The star was included in the study by Kallinger et al. (2019). BTr data are of good quality, but UBr and BLb data sets are short and scarce.

HD 189178 (Field 10): No variability was detected in the short BTr data set.

HD 189687 (25 Cyg, Fields 4 & 10): Known Be star. *Field 4:* Observed with BLb. The data set is short and scarce, but shows the evidence of weak variability. *Field 10:* Observed with BTr and UBr. Twelve days of BTr data show clear and complex variability. The 17 days long UBr light curve has inferior quality and does not show the variability. The strongest signal in the FS of these data is at 1.76 d^{-1}.

HD 189849 (15 Vul, Field 10): Observed with BAb, BTr and UBr. No variability was detected in UBr and BTr data. The BAb light curve is scarce and of poor quality.

HD 191610 (28 Cyg, Fields 4 & 10): This is a known Be star. *Field 4:* Observed with BTr and BLb. The data sets are short and scarce, but show some complex variability. *Field 10:* Observed with BLb, UBr and BTr. The FSa of the data reveal complex Be-type variability with the main peak at a frequency of 1.377 d^{-1}. The BRITE data for this star have been studied in detail by Baade et al. (2018a).

HD 192577/8 (31 Cyg, Fields 4 & 10): *Field 4:* Observed with BTr, UBr and BLb. The BTr data reveal complex variability. The UBr and BLb data sets are short and scarce. *Field 10:* No variability was detected in the scarce BLb and BAb data sets.

HD 192640 (29 Cyg, Fields 4 & 10): Known δ Sct-type variable. *Field 4:* Observed with BTr and BLb. The FSa of the data show many peaks at frequencies typical for a δ Sct star, the highest lies at a frequency of 37.4 d^{-1}. *Field 10:* Observed with BAb, BTr and UBr. A very similar to Field 4 δ Sct-type variability can be seen in these data.

HD 192685 (QR Vul, Field 10): Observed with BTr, BLb and UBr. The FS of the 156-d long BTr data shows strong and complex variability with the main peak at a frequency of 0.195 d^{-1}. The BLb data set is short and UBr data set is of poor quality.

HD 192806 (23 Vul, Field 4): Observed with BTr. The data do not show any prominent variability, but several low-frequency peaks can be seen in their FS.

HD 192909/10 (o Cet, Field 4): Observed with BTr and UBr. The BTr light curve shows some strong and complex variability. No variability was detected in the short and scarce UBr data set.

HD 193092 (Field 4): No variability was detected in the BTr data.

HD 193237 (P Cyg, Fields 4 & 10): Blue supergiant with known variability. *Field 4:* Observed with BTr, BLb and UBr. The BTr and BLb light curves show strong variability. The UBr data set is short and scarce. *Field 10:* Observed with BTr, UBr, BLb and BAb. The BTr data show clear variability. The UBr, BLb and BAb data sets are shorter. The BRITE data for this star were investigated in detail by Elliott et al. (2022).

HD 194093 (γ Cyg, Fields 4 & 10): *Field 4:* Observed with BTr, BLb and UBr. The BTr light curve shows some low-amplitude long-term variability, while the BLb data do not reveal any variability. The UBr data set is short and scarce. *Field 10:* No variability was detected in the UBr, BAb and BLb data.

HD 194317 (39 Cyg, Field 4): Observed with BTr and UBr. The FS of the BTr data reveals a significant peak at a frequency of 0.76 d^{-1}. The UBr data set is short and scarce.

HD 194335 (Field 10): Known Be star. No variability was detected in the BLb data.

HD 195068/9 (43 Cyg, Field 10): Observed with BTr and BLb. The FS of the BTr data clearly shows γ Dor-type pulsations with the main frequency at 1.25 d^{-1}. No variability was detected in the short BLb data set. The star was studied in detail by Zwintz et al. (2017).

HD 195295 (41 Cyg, Fields 4 & 10): *Field 4:* No variability was detected in the BTr, UBr and BLb data. *Field 10:* No variability was detected in the UBr data.

HD 195556 (ω^1 Cyg, Field 10): Observed with BAb and BTr. The BAb data set is of poor quality. The BTr data set is only 12.4 days long and shows evidence of long-term variability.

HD 196093/4 (47 Cyg, Field 4): Observed with BTr and UBr. The BTr data show complex variability. The UBr data set is scarce.

HD 197345 (α Cyg, Fields 4 & 10): *Field 4:* Observed with BTr, BLb and UBr. The FSa of the BTr and BLb data show clear variability at low frequencies; the UBr data set is scarce. *Field 10:* Observed with UBr, BAb and BLb. The FSa of the data show variability at low frequencies.

HD 197912 (52 Cyg, Field 4): No variability was detected in the short BTr and in the short and scarce BLb and UBr data sets.

HD 197989 (ε Cyg, Fields 4 & 10): *Field 4:* No variability was detected in the BLb and BTr data or in the short and scarce UBr data set. *Field 10:* No variability was detected in the BAb, BLb and UBr data. The star was included in the study by Kallinger et al. (2019).

HD 198183 (λ Cyg, Fields 4 & 10): *Field 4:* Observed with BLb, UBr and BTr. The BLb and UBr data sets are short. The BTr data show complex variability. *Field 10:* Observed with BTr, UBr, BLb and BAb. A complex variability is clearly present in the BTr data and less evident in the UBr data. The BAb data set is of poor quality, the BLb data set is short.

HD 198478 (55 Cyg, Fields 4 & 10): *Field 4:* Observed with BTr and BLb. The FS of the BTr data shows complex low-frequency variability. The BLb data set is short and scarce. *Field 10:* Observed with BTr, BAb, UBr and BLb. The BTr light curve shows complex variability which is less evident in the BAb light curve due to the sparsity and low quality of the data. The FS of the UBr data shows low-frequency variability. The BLb data set is short.

HD 198639 (56 Cyg, Field 10): No variability was detected in the BTr or BAb data.

HD 198726 (T Vul, Fields 4 & 10): Classical Cepheid. *Field 4:* Observed with BTr and UBr. The BTr light curve shows variability with a period of ∼4.44 d. The UBr data set is shorter, but the variability is clearly detectable despite the sparsity of the data. *Field 10:* Observed with BTr. The light curve shows variability with the same period as in the Field 4 observations.

HD 198809 (31 Vul, Field 4): The UBr data set is short and scarce. No variability was detected.

HD 199081 (57 Cyg, Fields 4 & 10): *Field 4:* Observed with BLb and BTr. The FSa of the data show strong frequency at 0.934 d^{-1}. *Field 10:* Observed with BTr, BAb, UBr and BLb. The FS of the BTr data shows multiple frequencies below ∼1.1 d^{-1}; the strongest peak is at a frequency of 0.934 d^{-1}. The BAb and UBr data sets are shorter, but the low-frequency variability is confirmed in their FSa. The BLb data set is of poor quality.

HD 199629 (ν Cyg, Fields 4 & 10): *Field 4:* No variability was detected in the UBr data. *Field 10:* No variability was detected in the UBr data.

HD 200120 (59 Cyg, Fields 4 & 10): Known Be star. *Field 4:* No variability was detected in the short and scarce BLb data set. *Field 10:* Observed with BTr, BAb and BLb. The FS of the BTr data shows clear variability with frequencies between ∼1.5 and 2.2 d^{-1}. The BAb and BLb data sets are short and scarce.

HD 200310 (60 Cyg, Field 10): Known Be star, observed with BTr, BAb and BLb. The FS of the BTr data shows clear variability with frequencies below 4 d^{-1}. The BAb data set is shorter and of poorer quality. The BLb data set is scarce.

HD 200905 (ξ Cyg, Field 4): Observed with BTr and UBr. The BTr light curve shows variability with a period of ∼17.3 d. No variability was detected in the short and scarce UBr data set.

HD 201078 (DT Cyg, Fields 4 & 10): Classical Cepheid. *Field 4:* Observed with BTr and UBr. The light curves show classical Cepheid variability with a period of ∼2.5 d. *Field 10:* Observed with BTr and BLb. The BTr light curve shows variability with the same period as the Field 4 data. The BLb light curve is short, but the variability can also be seen.

HD 201251 (63 Cyg, Field 4): No variability was detected in the BTr data or in the short and scarce UBr data set.

HD 201433 (V389 Cyg, Field 10): This is a triple system with SPB pulsations, observed with BTr and BLb. The BTr light curve shows SPB-type pulsations, confirmed also in the BLb data despite their scarcity. The BRITE data of this star were discussed in detail by Kallinger et al. (2017).

HD 202109 (ζ Cyg, Fields 4 & 10): *Field 4:* No variability was detected in the BLb and BTr data or in the short and scarce UBr data sets. *Field 10:* No variability was detected in the UBr and BAb data or in the short and scarce BLb data set.

HD 202444 (τ Cyg, Fields 4 & 10): *Field 4:* No variability was detected in the BLb and BTr data or in the short and scarce UBr data set. *Field 10:* No variability was detected in the BAb data or in the short and scarce BLb data set.

HD 202850 (σ Cyg, Fields 4 & 10): *Field 4:* Observed with BTr, BLb and UBr. The FSa of the BTr and BLb data show some low-frequency variability. The UBr data set is short and scarce. *Field 10:* Observed with BAb, BLb and BTr. The FS of the BTr data shows low-frequency variability. The BAb and BLb data sets are shorter and scarce.

HD 202904 (υ Cyg, Fields 4 & 10): Known Be star. *Field 4:* Observed with BTr, BLb and UBr. The FS of the BTr data shows strong variability at very low frequencies. The FS of the BLb data reveals a frequency of ∼1.47 d^{-1} on the top of the lower frequency variability. The UBr data set is short and scarce. *Field 10:* Observed with BTr, BAb and BLb. The FS of the BTr data shows clear variability with a frequency of 1.47 d^{-1}. The BAb and BLb data sets are shorter and scarce.

HD 203064 (68 Cyg, Fields 4 & 10): *Field 4:* No variability was detected in the BTr and BLb data. *Field 10:* No variability was detected in the BTr data or in the short and scarce BAb and BLb data sets.

HD 203156 (V1334 Cyg, Fields 4 & 10): Known classical Cepheid. *Field 4:* Observed with BTr and UBr. The light curves clearly show variability with a period of ∼3.3 d. *Field 10:* Observed with BTr and BLb. The variability seen in the Field 4 data is confirmed in the BTr data set. The BLb data set is short and scarce.

HD 203280 (α Cep, Field 11): No variability was detected in the short BLb data set.

HD 205021 (β Cep, Field 11): The BHr and BLb data sets are very sparse and not useful for scientific analysis.

HD 205435 (ρ Cyg, Field 10): No variability was detected in the good-quality BTr and UBr data or in the short and scarce BLb data set.

HD 206570 (V460 Cyg, Field 4): No variability was detected in the BTr data.

HD 207260 (ν Cep, Field 11): Observed with BHr and BLb. The FS of the BHr data shows weak low-frequency variability. The BLb data set is short and of lower precision.

HD 209790 (ξ Cep, Field 11): No variability was detected in the BHr data and in the short BLb data set.

HD 209975 (19 Cep, Field 11): Observed with BHr and BLb. The FSa of the BHr data show some stochastic low-frequency variability. The BLb data set is short and scarce.

HD 210745 (ζ Cep, Field 11): No variability was detected in the BHr data.

HD 211336 (ε Cep,Field 11): Known δ Sct-type pulsator, observed with BTr, BLb and BHr. The FSs of the BTr and BLb data show δ Sct-type variability. The BHr data set is short and not usable.

HD 213306 (δ Cep, Field 11): This is the prototype of classical Cepheids. Observed by BTr, BLb and BHr. The data are of excellent quality and show variability with a period of ∼5.4 d.

HD 216228 (ι Cep, Field 11): No variability was detected in the relatively short BHr data set.

HD 218376 (1 Cas, Field 11): No variability was detected in the short BLb and BHr data sets.

HD 220652 (4 Cas, Field 11): Observed with BHr. The data set is short and its FS shows some low-frequency variability.

HD 221253 (AR Cas, Field 11): Known eclipsing and spectroscopic binary. Observed with BLb and BHr. The light curves show clear eclipses with an orbital period of ~6.1 d.

HD 224572 (σ Cas, Field 11): No variability was detected in the BAb data set.

HD 225289 (V567 Cas, Field 11: No variability was detected in the short BHr data set.

Appendix C: Format of BRITE-Constellation data in the archives

Appendix C.1: Contents of the BRITE-Constellation data in the archives

All decorrelated BRITE-Constellation data described and illustrated in this article are freely available for download from the BRITE Public Data Archive (PDA)[2] and the Canadian Astronomy Data Centre (CADC)[3].

Both databases provide the data as ASCII files split into setups (explained in Appendix C.2). For each setup, five different files are available. They contain the original time series (i.e., before the decorrelation procedure), the decorrelated time series, the time series containing averages per satellite orbit, the variability model used in the decorrelation, and the log file generated by the software during the decorrelation. All files have headers that describe their contents in detail. The files containing photometric time series (i.e., original, decorrelated and orbit averaged data) include columns with the Heliocentric or Barycentric Julian Date, instrumental magnitudes including errors and magnitudes with the mean instrumental magnitude of the given setup subtracted. Observations with the largest errors are filtered out during the decorrelation process. For further analyses, the provided errors in magnitudes can be used to filter the data if needed.

Appendix C.2: BRITE-Constellation photometry subrasters and setups

The following brief explanation of the subrasters and setups used for BRITE-Constellation observations provides essential guidance for a better understanding of BRITE-Constellation data. More details are given in Popowicz et al. (2017).

The full frame CCD images of the BRITE-Constellation satellites cannot be transferred to ground at the cadence taken in space which is typically about 20 s. Therefore, in the context of BRITE photometry, the expression 'subrasters' concerns the definition of which parts of the full frame CCD are rendered into images before transmitting to the ground. For that the (x, y) starting position on the CCD is provided and the x and y size of each subraster is required. In stare mode, those regions of interest or subrasters are 24×24 pixels in size, while in chopping mode they are rectangular and cover 24×48 pixels. Typically 15 to 30 subrasters are set up for each satellite and observing campaign. With a few exceptions, each subraster contains the profile of a single target in its central part in the case of stare mode. In chopping mode, a star is located either on one or the other side of the rectangular subraster. In addition to the positions of the subrasters, the exposure time and the time between exposures has to be specified as well as the central right ascension, declination and the roll angle with respect to the optical axis. It is important that the stellar profile and a number of neighbouring background areas are fully rendered in each subraster even when the pointing changes slightly from exposure to exposure.

Data obtained by a given satellite are split into parts, called setups. Each observing run starts with an initial setup number (1), which is the first attempt to acquire the selected stars properly in the defined subrasters. Very often this first setup needs to be changed or optimised, and, hence, a new setup is generated during an early phase of an observing campaign. Furthermore when stars (and new subrasters) are added or removed, a new setup is generated and uploaded to the respective satellite. During some observing runs, a slow drift on the orientation of a given satellite over time had been apparent and, therefore, a resetting of the subraster was needed in order to keep the stellar profiles well in range of the subraster borders. Also, a change in exposure time or observing cadence always results in a new setup. Hence, during a full campaign for each satellite several setups might have been utilized. In some cases only two or three were used to collect data over up to 180 d but it can be up to seven or more if needed. Data can also be split into setups during the initial reductions, that is on the ground (see Appendix A of Popowicz et al. (2017)).

New setups introduced during observations can have an effect on the integrity of a light curve (time, magnitude) after reduction and even decorrelation as described in this paper. When a new setup changes the position of the star in a subraster from (too) close to the border to centre (or accidentally in reverse), jumps in the signal levels can occur. Jumps can also occur as a result of the reduction, because each setup is processed independently and for each setup an independent aperture is defined. Therefore, if a setup covers only a short part of a long period variable star light curve, the reduction and decorrelation of such a small segment can result in serious offsets that do not reflect the real long-term variability of the object. If setups are generated during the initial process of data reduction, no offsets or other changes in data quality are introduced. In this case, the light curve is split only into two or more parts.

In particular during this first phase of the BRITE-Constellation mission, many individual setups were required for technical reasons (such as the very first observations conducted with the individual satellites that needed testing or the change from stare mode to chopping mode). In later years of the BRITE-Constellation mission, the number of setups decreased and were introduced more often by the reduction process that required splitting the data into parts.

Appendix C.3: Recommendations on combining individual setups and data sets from different BRITE satellites

The decorrelated photometric time series contain the Barycentric Julian date, instrumental magnitudes and magnitudes with the mean instrumental magnitude of the given setup subtracted (see the headers of the files stored in the archives for more information). In many cases, the time series stored as individual setups can just simply be stitched together (e.g., if the setups were generated during the reduction process) without any issues.

However, very often different setups can have different mean magnitudes which cause different offsets to be taken into account when combining them into a full light curve. A good example is shown in Figure 3 of the paper: individual setups are marked with vertical lines and the numbers on top of the light curve illustrate the offsets that were applied and the $\sigma^{\rm med}_{\rm orbit}$ parameter as a measure for the data quality.

There are some cases where combining different setups needs a bit more care. For any type of a long-period variable,

[2] https://brite.camk.edu.pl/pub

[3] https://www.cadc-ccda.hia-iha.nrc-cnrc.gc.ca/en/

for example, stitching together the time series with the mean magnitude subtracted will not yield a reliable result. Introducing individual offsets by adding constants to a given setup might be necessary to cover the intrinsic variability of the star.

Full light curves obtained by different BRITE satellites using the same filter can be combined by subtracting the mean magnitude from each light curve individually. Data taken in different BRITE filters can be combined after subtracting the mean magnitudes only if the amplitudes are expected to be similar in both bands or if the observations in one filter are scaled to the amplitude of the other.

Appendix D: Data quality per satellite

Figures D.1 to D.5 illustrate the noise properties for each of the five BRITE-Constellation instruments individually.

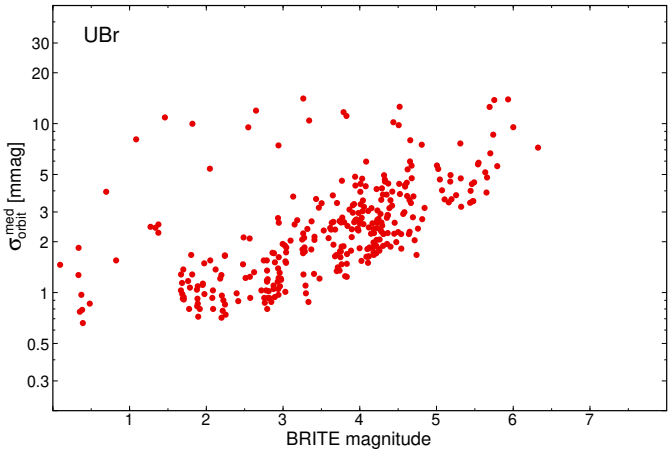

Fig. D.1: Values of σ^{med}_{orbit} plotted as a function of instrumental BRITE magnitude for UBr setups.

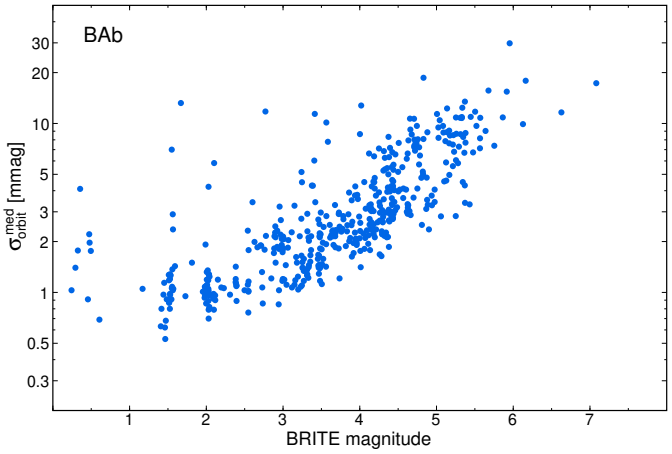

Fig. D.2: Values of σ^{med}_{orbit} plotted as a function of instrumental BRITE magnitude for BAb setups.

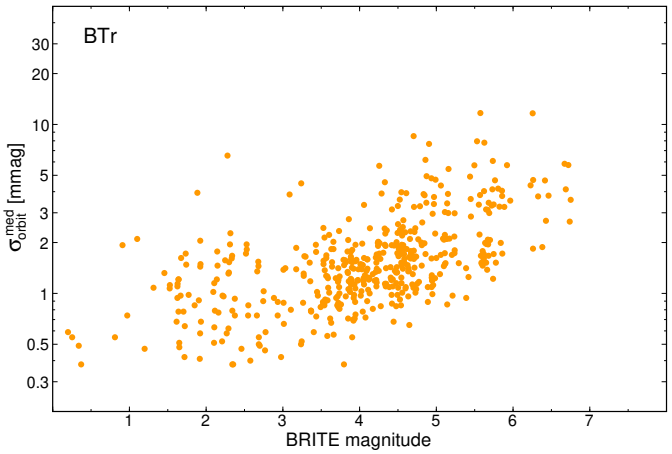

Fig. D.3: Values of σ^{med}_{orbit} plotted as a function of instrumental BRITE magnitude for BTr setups.

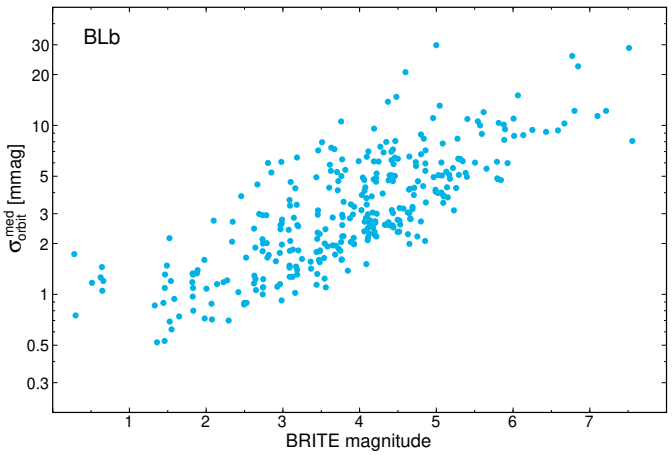

Fig. D.4: Values of σ^{med}_{orbit} plotted as a function of instrumental BRITE magnitude for BLb setups.

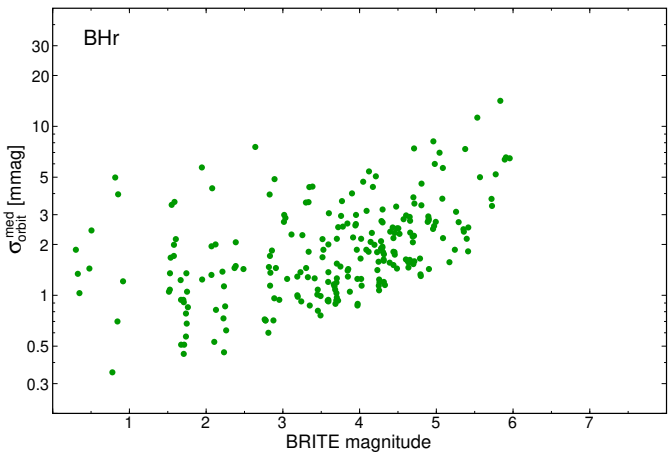

Fig. D.5: Values of σ^{med}_{orbit} plotted as a function of instrumental BRITE magnitude for BHr setups.

Appendix E: Field maps

Sky maps of the Fields 1 to 14 observed by BRITE-Constellation are shown in Figs. E.1, E.2 and E.3: Observed stars are marked as red filled circles where the size of the symbol corresponds to the magnitude. The black numbers next to those symbols are HD identifiers (see Table A.1). The names of the stellar constellations are given in blue.

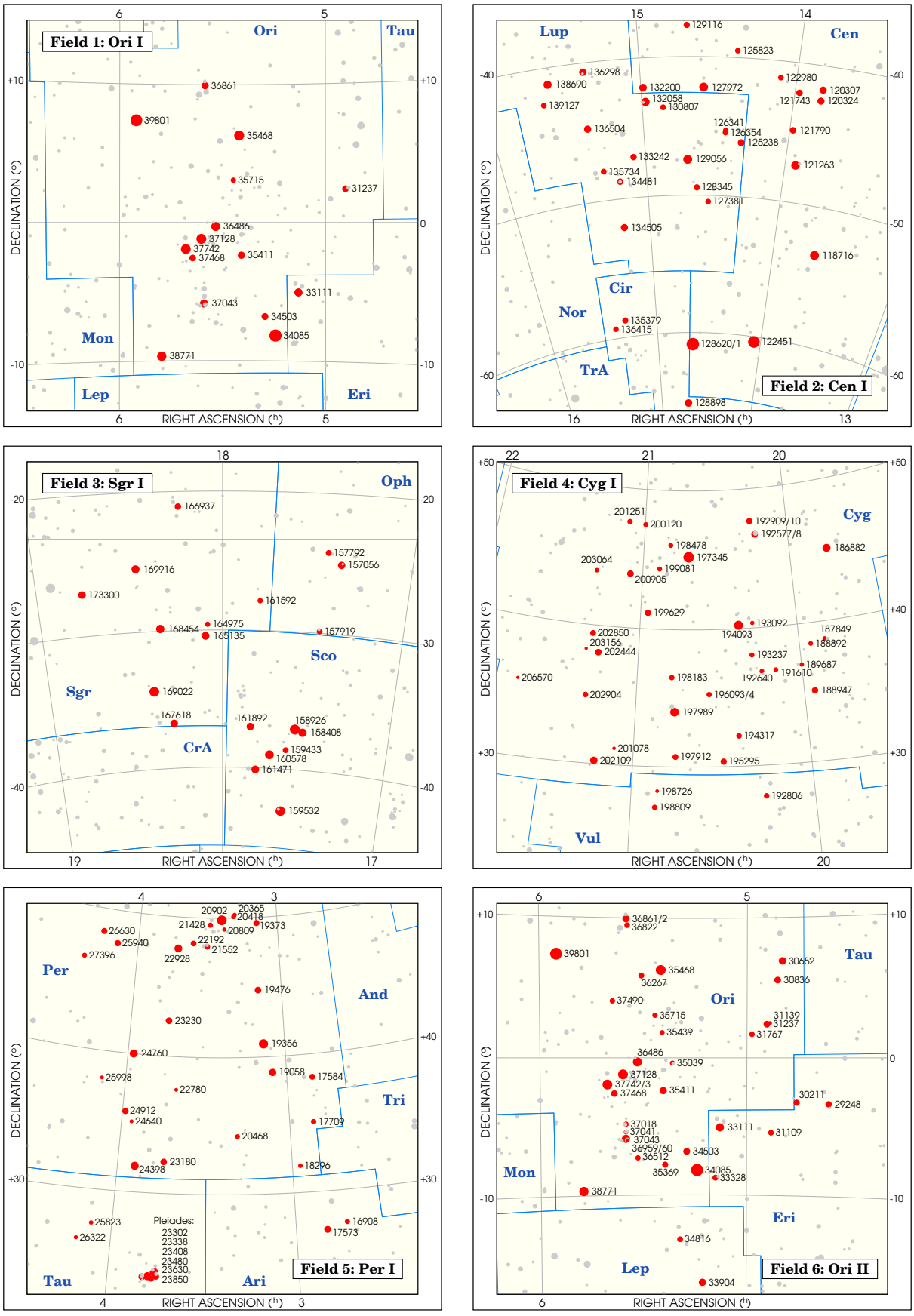

Fig. E.1: BRITE-Constellation field maps: Fields 1 to 6.

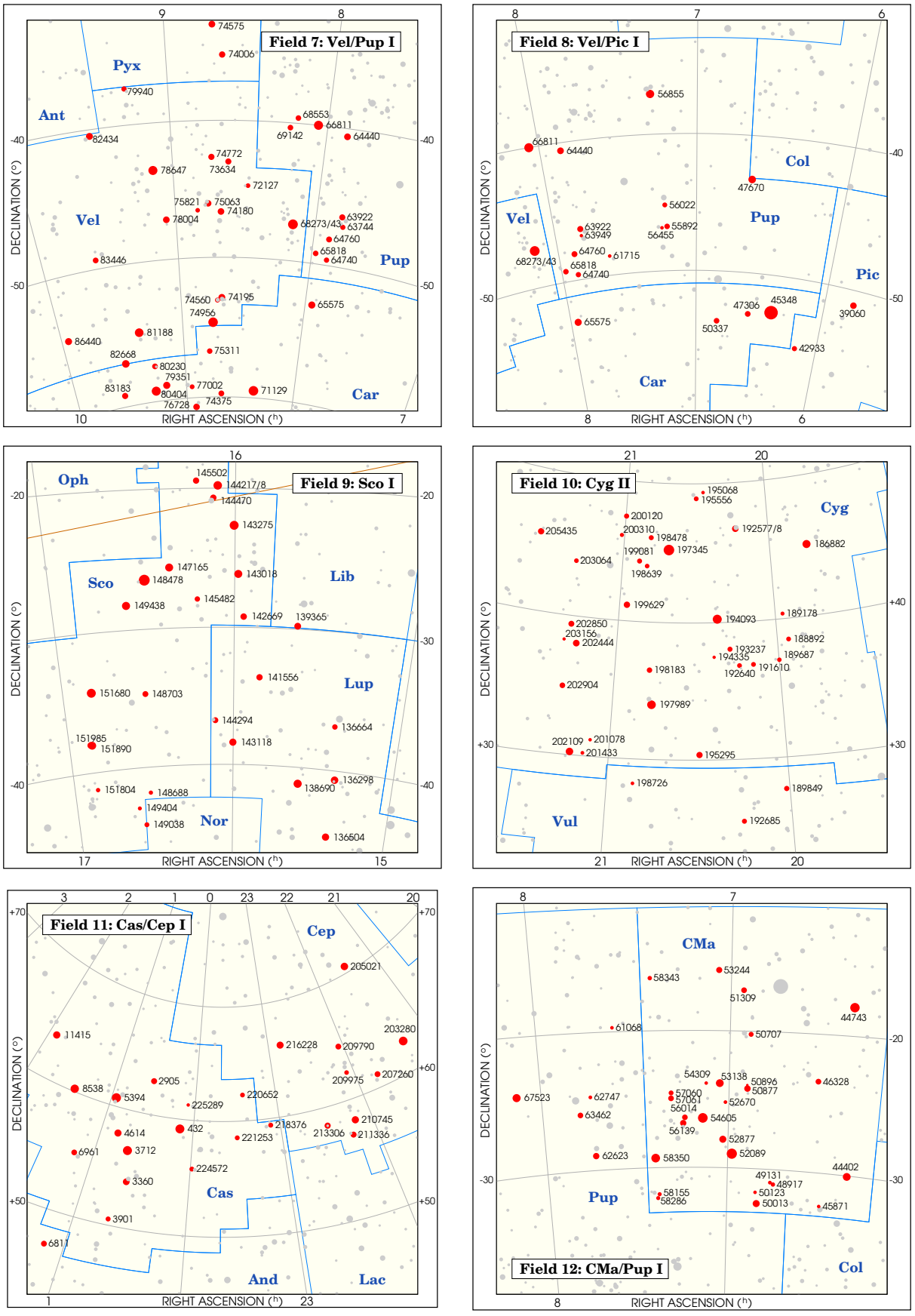

Fig. E.2: BRITE-Constellation field maps: Fields 7 to 12.

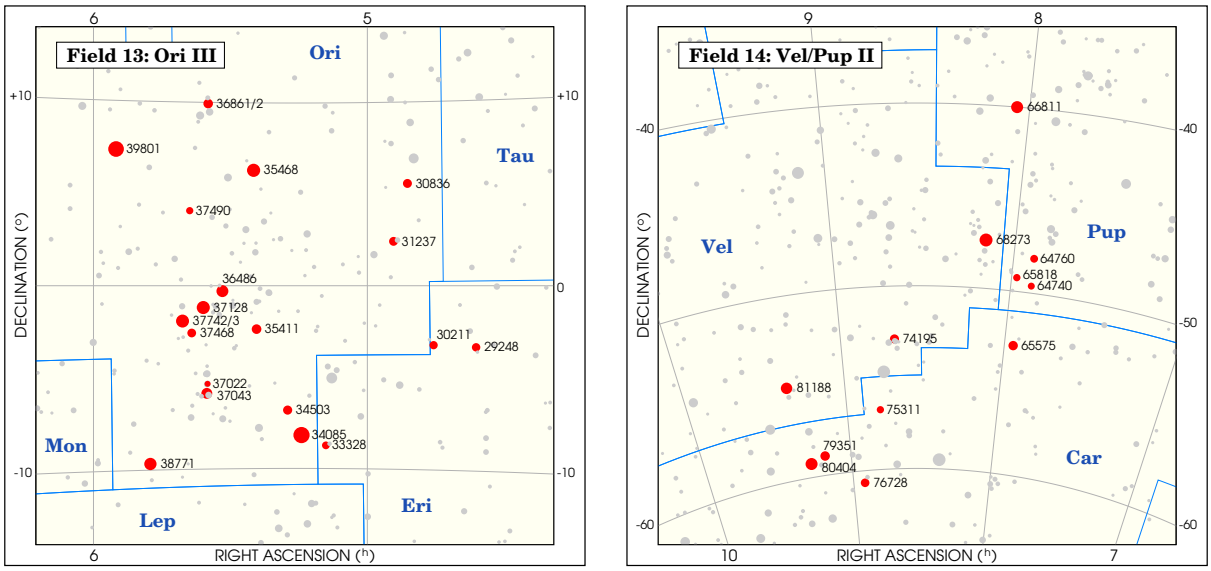

Fig. E.3: BRITE-Constellation field maps: Fields 13 and 14.